

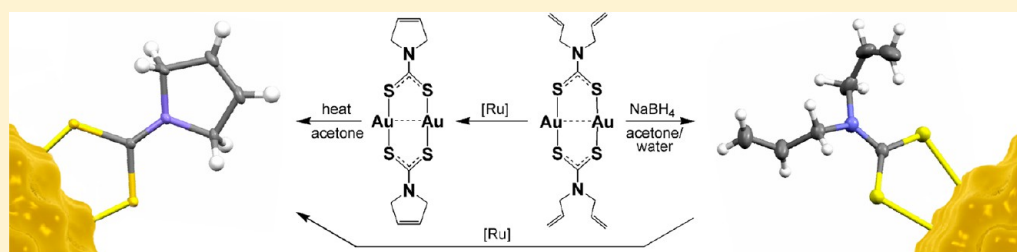
Ring-Closing Metathesis and Nanoparticle Formation Based on Diallyldithiocarbamate Complexes of Gold(I): Synthetic, Structural, and Computational Studies

Saira Naeem,[†] Stefano A. Serapian,[†] Anita Toscani,[†] Andrew J. P. White,[†] Graeme Hogarth,[‡] and James D. E. T. Wilton-Ely^{*,†}

[†]Department of Chemistry, Imperial College London, South Kensington Campus, London SW7 2AZ, U.K.

[‡]Department of Chemistry, University College London, 20 Gordon Street, London WC1H 0AJ, U.K.

Supporting Information



ABSTRACT: The gold(I) complexes $[\text{Au}\{\text{S}_2\text{CN}(\text{CH}_2\text{CH}=\text{CH}_2)_2\}(\text{L})]$ [$\text{L} = \text{PPh}_3, \text{PCy}_3, \text{PMe}_3, \text{CN}^t\text{Bu}, \text{IDip}$] are prepared from $\text{KS}_2\text{CN}(\text{CH}_2\text{CH}=\text{CH}_2)_2$ and $[(\text{L})\text{AuCl}]$. The compounds $[\text{L}_2(\text{AuCl})_2]$ ($\text{L}_2 = \text{dppa}, \text{dppf}$) yield $[(\text{L}_2)\{\text{Au}_2\text{S}_2\text{CN}(\text{CH}_2\text{CH}=\text{CH}_2)_2\}_2]$, while the cyclic complex $[(\text{dppm})\{\text{Au}_2\text{S}_2\text{CN}(\text{CH}_2\text{CH}=\text{CH}_2)_2\}]\text{OTf}$ is obtained from $[\text{dppm}(\text{AuCl})_2]$ and AgOTf followed by $\text{KS}_2\text{CN}(\text{CH}_2\text{CH}=\text{CH}_2)_2$. The compound $[\text{Au}_2\{\text{S}_2\text{CN}(\text{CH}_2\text{CH}=\text{CH}_2)_2\}_2]$ is prepared from $[(\text{tht})\text{AuCl}]$ ($\text{tht} = \text{tetrahydrothiophene}$) and the diallyldithiocarbamate ligand. This product ring-closes with $[\text{Ru}(\text{=CHPh})\text{Cl}_2(\text{SIMes})(\text{PCy}_3)]$ to yield $[\text{Au}_2(\text{S}_2\text{CNC}_4\text{H}_6)_2]$, whereas ring-closing of $[\text{Au}\{\text{S}_2\text{CN}(\text{CH}_2\text{CH}=\text{CH}_2)_2\}(\text{PR}_3)]$ fails. Warming $[\text{Au}_2\{\text{S}_2\text{CN}(\text{CH}_2\text{CH}=\text{CH}_2)_2\}_2]$ results in formation of gold nanoparticles with diallyldithiocarbamate surface units, while heating $[\text{Au}_2(\text{S}_2\text{CNC}_4\text{H}_6)_2]$ with NaBH_4 results in nanoparticles with 3-pyrroline dithiocarbamate surface units. Larger nanoparticles with the same surface units are prepared by citrate reduction of HAuCl_4 followed by addition of the dithiocarbamate. The diallyldithiocarbamate-functionalized nanoparticles undergo ring-closing metathesis using $[\text{Ru}(\text{=CHC}_6\text{H}_4\text{O}^i\text{Pr}-2)\text{Cl}_2(\text{SIMes})]$. The interaction between the dithiocarbamate units and the gold surface is explored using computational methods to reveal no need for a counteranion. Preliminary calculations indicate that the Au–S interactions are substantially different from those established in theoretical and experimental studies on thiolate-coated nanoparticles. Structural studies are reported for $[\text{Au}\{\text{S}_2\text{CN}(\text{CH}_2\text{CH}=\text{CH}_2)_2\}(\text{PPh}_3)]$ and $[\text{Au}_2\{\text{S}_2\text{CN}(\text{CH}_2\text{CH}=\text{CH}_2)_2\}_2]$. In the latter, exceptionally short intermolecular aurophilic interactions are observed.

INTRODUCTION

Highly active catalysts with good functional group tolerance have made alkene metathesis a powerful and accessible tool in synthetic organic chemistry.¹ Ring-closing metathesis (RCM) can be used to create a range of small or medium-sized rings, including heterocycles.² Some substrates remain problematic, such as species that are capable of binding to the vacant site of the coordinatively unsaturated precatalysts of the Grubbs type. Unprotected amines may be considered in this group of substrates due to the competition for coordination to the metal between the amine lone pair and the alkene. This can be overcome by employing electron-withdrawing substituents on the amine to favor alkene coordination.^{3a,3b} An allied approach is the use of Lewis acids such as $\text{Ti}(\text{O}^i\text{Pr})_4$ to coordinate the lone pair before metathesis is carried out.^{3c}

Although dithiocarbamate complexes of transition metals have been known for more than a hundred years,⁴ the NR_2

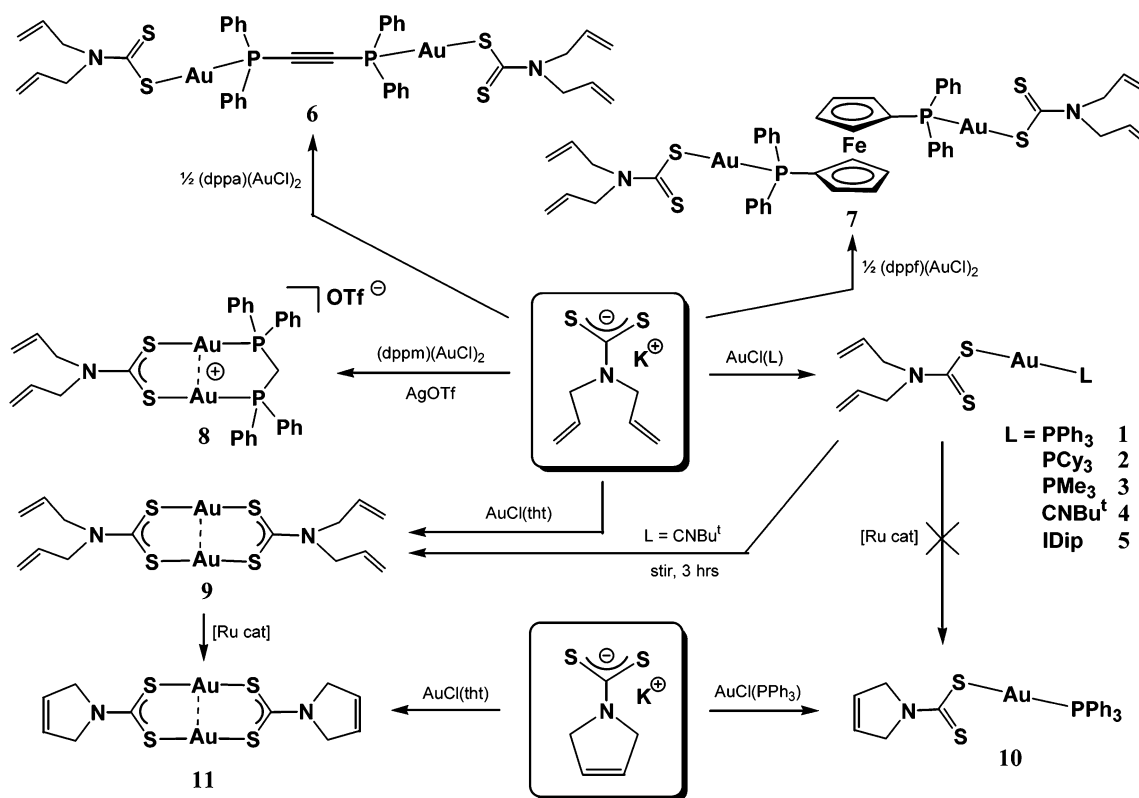
substituents are often overlooked as a source of further reactivity.⁵ Our recent work has sought to exploit this potential while making use of the well-established attributes of dithiocarbamates, such as their stabilization of a wide range of oxidation states.⁶ In the context of this interest in functionalized sulfur-based ligands,^{7,8} we have recently explored an alternative means of modifying amines with alkene functionality for metathesis by their incorporation into a dithiocarbamate ligand, R_2NCS_2^- . Thus, a wide range of metal complexes of diallyldithiocarbamate undergo RCM catalyzed by $[\text{Ru}(\text{=CHPh})\text{Cl}_2(\text{SIMes})(\text{PCy}_3)]$, including some bearing surprisingly sterically bulky coligands.⁹

Sporadic reports of examples of (mostly homoleptic) metal complexes of the diallyldithiocarbamate ligand have appeared in

Received: August 8, 2013

Published: February 10, 2014

Scheme 1. [Ru cat] = 10 mol % [Ru(=CHPh)Cl₂(SIMes)(PCy₃)]; SIMes = 1,3-bis(2,4,6-trimethylphenyl)imidazolidin-2-ylidene; IDip = 1,3-bis(2,6-diisopropylphenyl)imidazol-2-ylidene



the literature.¹⁰ However, for gold, only complexes in the trivalent state are known,¹¹ despite gold(I) and gold(II) complexes of other dithiocarbamates being numerous. Indeed, some of the first examples of divalent gold were observed in dithiocarbamate compounds.^{5d,11b}

In extending the exploration of the coordination and subsequent reactivity of the diallyldithiocarbamate ligand to gold(I) complexes, we have discovered that the chemistry of these complexes departs significantly from that found for the complexes with metals earlier in the transition series. Furthermore, some of these compounds provide access to gold nanoparticles from molecular dithiocarbamate precursors in an unexpectedly facile and unprecedented fashion. Since the first reports by Wessels,^{12a} Wei,^{12b} and Beer,^{12c} the use of dithiocarbamates for the surface functionalization of gold nanoparticles has received increasing attention.^{8a-c,12d-s} We also report the first computational studies to probe the interaction of the dithiocarbamate unit and the gold surface, which contrasts substantially from what is observed in thiolate-coated nanoparticles of gold.

RESULTS AND DISCUSSION

Synthesis of Diallyldithiocarbamate Complexes. In all reactions, the diallyldithiocarbamate ligand was generated in situ from diallylamine and a slight excess of KOH and carbon disulfide. This solution was used immediately before any precipitation of the ligand could occur. An acetone-dichloromethane solution of [(Ph₃P)AuCl] was treated with 1.1 equiv of K₂S₂CN(CH₂CH=CH₂)₂ to yield a yellow product in excellent yield. Mass spectrometry (molecular ion at *m/z* = 632) and elemental analysis supported the formation of [(Ph₃P)Au{S₂CN(CH₂CH=CH₂)₂}] (1), formed through

displacement of the chloride ligand by the dithiocarbamate donor (Scheme 1). A new singlet was observed in the ³¹P NMR spectrum, while analysis by ¹H NMR spectroscopy revealed three multiplet resonances not present in the precursor at 4.59 ppm (NCH₂ protons), 5.25 ppm (H^{A,B}), and 5.98 ppm (H^C), using the numbering scheme in Figure 1. In this example,

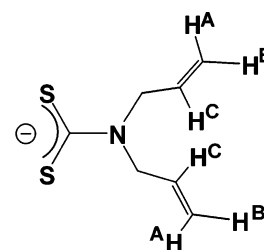


Figure 1. The diallyldithiocarbamate ligand employed in this Work, showing the numbering scheme used for spectroscopic purposes.

discrete couplings could not be reliably identified. ¹³C NMR analysis revealed a resonance at 209.0 ppm for the CS₂ carbon, while the diallyl ligand gave rise to resonances at 132.2 (=CH₂), 118.0 (CH₂C), and 56.4 (NCH₂) ppm. To complete the characterization of this molecule, single crystals were grown by vapor diffusion of diethyl ether onto a solution of 1 in dichloromethane. A crystal was chosen for a structural study (Figure 2)—see Structural Discussion for further details.

The complexes [(Cy₃P)Au{S₂CN(CH₂CH=CH₂)₂}] (2) and [(Me₃P)Au{S₂CN(CH₂CH=CH₂)₂}] (3) were also prepared, bearing phosphines with greater and smaller steric bulk, respectively, than triphenylphosphine. In contrast to the case for 1, the coupling between the allyl protons in the ¹H

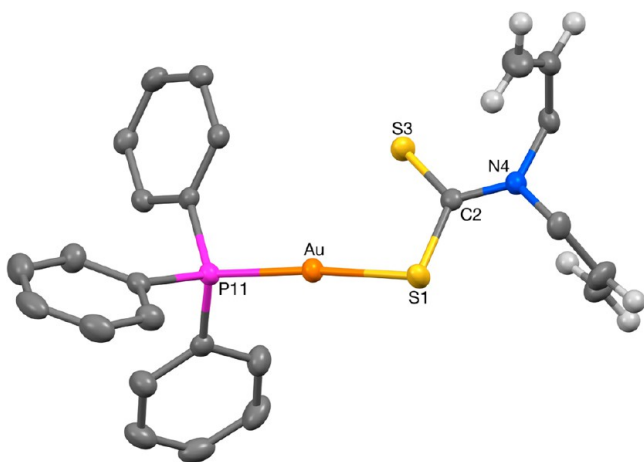


Figure 2. The molecular structure of **1** (50% probability ellipsoids). Selected bond lengths (Å) and angles (deg); Au–S(1) 2.3456(4), Au–P(11) 2.2517(4), S(1)–C(2) 1.7436(17), C(2)–S(3) 1.6971(17), C(2)–N(4) 1.341(2), S(1)–Au–P(11) 174.980(16), S(1)–C(2)–S(3) 119.97(10).

NMR spectrum was observed clearly in complex **2**, with the NCH₂ protons resonating at 4.54 ppm as a doublet ($J_{\text{HH}} = 5.8$ Hz). The doublets of doublets at 5.22 and 5.25 ppm were attributed to the terminal olefinic protons H^A ($J_{\text{HAHC}} = 15.9$ Hz) and H^B ($J_{\text{HBHC}} = 8.8$ Hz), respectively, and showed a mutual coupling of 1.4 Hz. The remaining allyl proton (H^C) was observed as a multiplet at 5.97 ppm. Similar spectroscopic features were observed in the ¹H NMR spectrum of [(Me₃P)Au{S₂CN(CH₂CH=CH₂)₂}] (**3**) along with a doublet for the protons of the trimethylphosphine ligand ($J_{\text{HP}} = 11.0$ Hz).

Although phosphine ligands are the most common nonsulfur donors in gold(I) chemistry, isocyanide ligands have been shown to act as good ligands in many cases. Their relatively undemanding steric profile (^tBuNC, ⁱPrNC, etc.) has led to an

interesting structural diversity, through the creation of favorable conditions for aurophilic contacts in the solid state.¹³

With this in mind, yellow [(^tBuNC)Au{S₂CN(CH₂CH=CH₂)₂}] (**4**) was prepared from [(^tBuNC)AuCl] and K₂S₂CN(CH₂CH=CH₂)₂. The isocyanide ligand was identified from the ν_{CN} absorption at 2203 cm⁻¹ in the solid-state IR spectrum and a singlet at 0.53 ppm in the ¹H NMR spectrum, in addition to typical resonances for the dithiocarbamate ligand. No molecular ion was observed in either electrospray or fast atom bombardment (FAB) mass spectra, although a fragmentation was observed in the latter for [M – ^tBuNC]⁺ at m/z 369. Although care must be taken when correlating reactivity with the fragmentations observed in the high-energy environment of a mass spectrometer, the apparent loss of isocyanide is also manifested in solution. Over a few hours in solution, a yellow precipitate was observed, which was later identified as the homoleptic complex, [Au₂{S₂CN(CH₂CH=CH₂)₂}] (**9**).

To broaden the range of coligands investigated, in particular from a steric viewpoint (metathesis studies), [(IDip)Au{S₂CN(CH₂CH=CH₂)₂}] (**5**) was prepared in good yield from [(IDip)AuCl] using the same method. Typical resonances for the dithiocarbamate ligand were observed in the ¹H NMR spectrum alongside doublets (1.25, 1.41 ppm) and a septet for the isopropyl substituents of the IDip ligand. Also observed were resonances at 7.38 and 7.53 ppm for the aromatic protons, while the HC=CH unit gave rise to a singlet resonance at 7.77 ppm. The overall formulation was confirmed by elemental analysis and mass spectrometry (FAB, +ve mode).

Following the successful preparation of monometallic compounds, attention turned to the synthesis of a number of digold complexes with the diallyldithiocarbamate ligand. Because of the rigidity of the 1,2-bis(diphenylphosphino)acetylene ligand, the complex [dppa(AuCl)₂] is ideal for the preparation of linear digold compounds, which cannot show intramolecular Au⋯Au contacts. This is the case for bright yellow [(dppa){AuS₂CN(CH₂CH=CH₂)₂}₂] (**6**), formed by treatment of [dppa(AuCl)₂] with 2.2 equiv of the diallyldithiocarbamate ligand (Scheme 1). Spectroscopic data for the

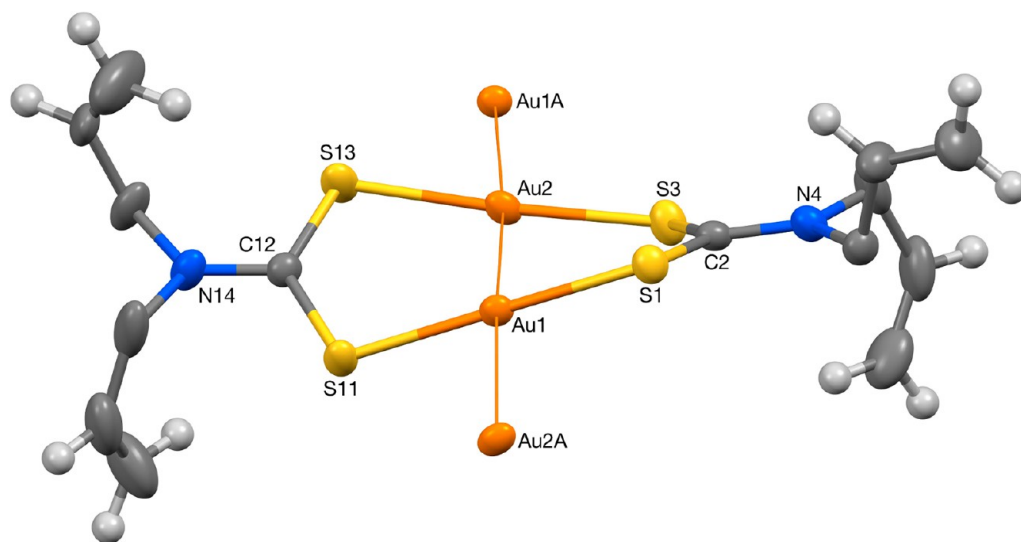


Figure 3. The molecular structure of **9** (50% probability ellipsoids). Selected bond lengths (Å) and angles (deg); Au(1)–S(1) 2.2913(8), Au(1)–S(11) 2.2967(8), Au(2)–S(3) 2.2958(9), Au(2)–S(13) 2.2950(9), S(1)–C(2) 1.728(3), C(2)–S(3) 1.731(3), C(2)–N(4) 1.338(4), S(11)–C(12) 1.734(3), C(12)–S(13) 1.727(3), C(12)–N(14) 1.330(4), Au(1)⋯Au(2) 2.79030(15), Au(1)⋯Au(2A) 2.98997(15), Au(2)⋯Au(1A) 2.98997(15), S(1)–Au(1)–S(11) 177.10(3), S(3)–Au(2)–S(13) 176.41(3), S(1)–C(2)–S(3) 127.1(2), S(11)–C(12)–S(13) 126.5(2).

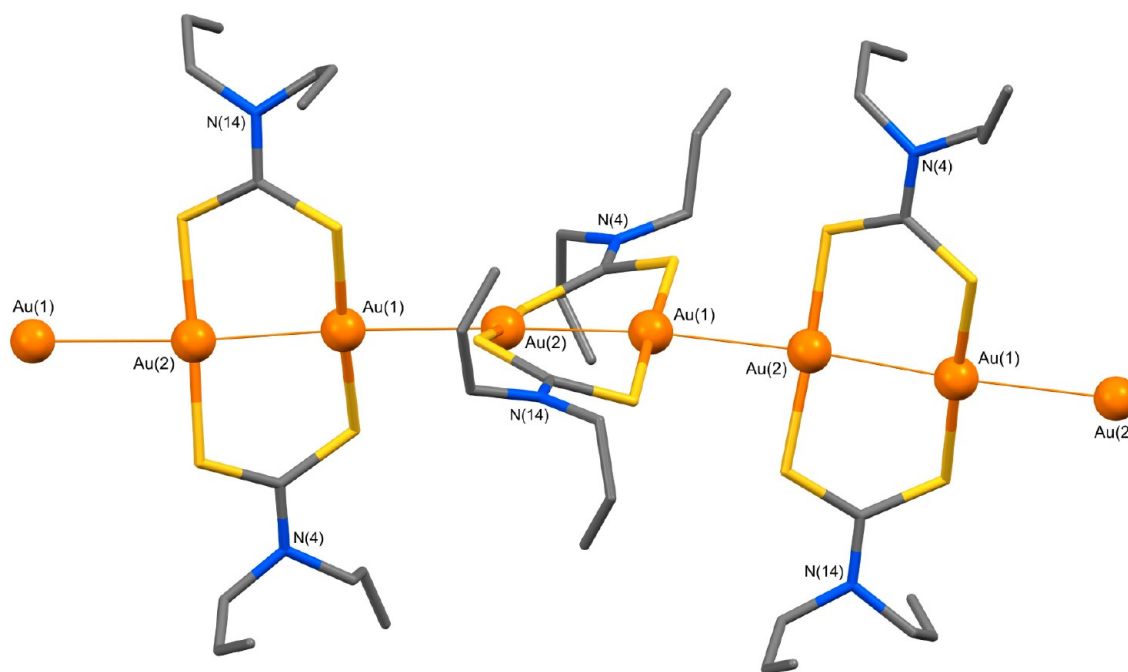


Figure 4. Part of one of the chains of 4_1 -screw related molecules that extend along the crystallographic c axis present in the structure of **9**. The intra- and intermolecular Au...Au separations are 2.79030(15) and 2.98997(15) Å, respectively.

dithiocarbamate ligand were similar to the complexes discussed above, while the presence of two “ $\text{AuS}_2\text{CN}(\text{CH}_2\text{CH}=\text{CH}_2)_2$ ” units was confirmed by mass spectrometry (molecular ion at m/z 1133) and good agreement of elemental analysis with calculated values. Reaction between $[(\text{dppf})(\text{AuCl})_2]$ and 2.2 equiv of $\text{KS}_2\text{CN}(\text{CH}_2\text{CH}=\text{CH}_2)_2$ yielded a pale yellow compound in 80% yield. In contrast to **6**, the flexibility afforded by the ferrocenyl unit suggested the possibility of a metallacyclic complex, $[(\text{dppf})\text{Au}_2(\mu_2\text{-S}_2\text{CN}(\text{CH}_2\text{CH}=\text{CH}_2)_2)]^+$, which was supported by the major peak in the FAB mass spectrum at m/z 1120. However, integration of the cyclopentadienyl resonances at 4.49 and 4.92 ppm in the ^1H NMR spectrum with those which are characteristic of the diallyldithiocarbamate ligand ruled out this possibility, as did the elemental analysis values. Thus, the product was formulated as $[(\text{dppf})\{\text{AuS}_2\text{CN}(\text{CH}_2\text{CH}=\text{CH}_2)_2\}_2]$ (**7**, Scheme 1). However, a metallacyclic compound was successfully obtained from $[(\text{dppm})(\text{AuCl})_2]$. The resulting product was initially isolated in poor yield from direct reaction of 1 equiv of the dithiocarbamate with this precursor. This synthesis was replaced by an improved route in which the chloride ligands were abstracted with silver triflate prior to addition of $\text{KS}_2\text{CN}(\text{CH}_2\text{CH}=\text{CH}_2)_2$. The product $[(\text{dppm})\text{Au}_2\{\text{S}_2\text{CN}(\text{CH}_2\text{CH}=\text{CH}_2)_2\}]\text{OTf}$ (**8**) gave rise to similar spectroscopic features to those found in the previous complexes, apart from a multiplet at 4.74 ppm for the PCH_2P protons. Unfortunately, none of these complexes proved sufficiently crystalline for an X-ray diffraction study.

As mentioned above, $[(^t\text{BuNC})\text{Au}\{\text{S}_2\text{CN}(\text{CH}_2\text{CH}=\text{CH}_2)_2\}]$ (**4**) was found to lose the isocyanide ligand in solution to form the homoleptic complex $[\text{Au}_2\{\text{S}_2\text{CN}(\text{CH}_2\text{CH}=\text{CH}_2)_2\}_2]$ (**9**). A more direct synthesis of **9** was provided by reaction of equimolar quantities of $[(\text{tht})\text{AuCl}]$ (tht = tetrahydrothiophene) and $\text{KS}_2\text{CN}(\text{CH}_2\text{CH}=\text{CH}_2)_2$ (Scheme 1). The spectroscopic and analytical data were unremarkable but confirm the identity of the product. To

explore the properties of this compound further, single crystals were grown by vapor diffusion of diethyl ether into a dichloromethane solution of the complex. A suitable crystal was chosen for a structural determination (Figure 3 and Structural Discussion).

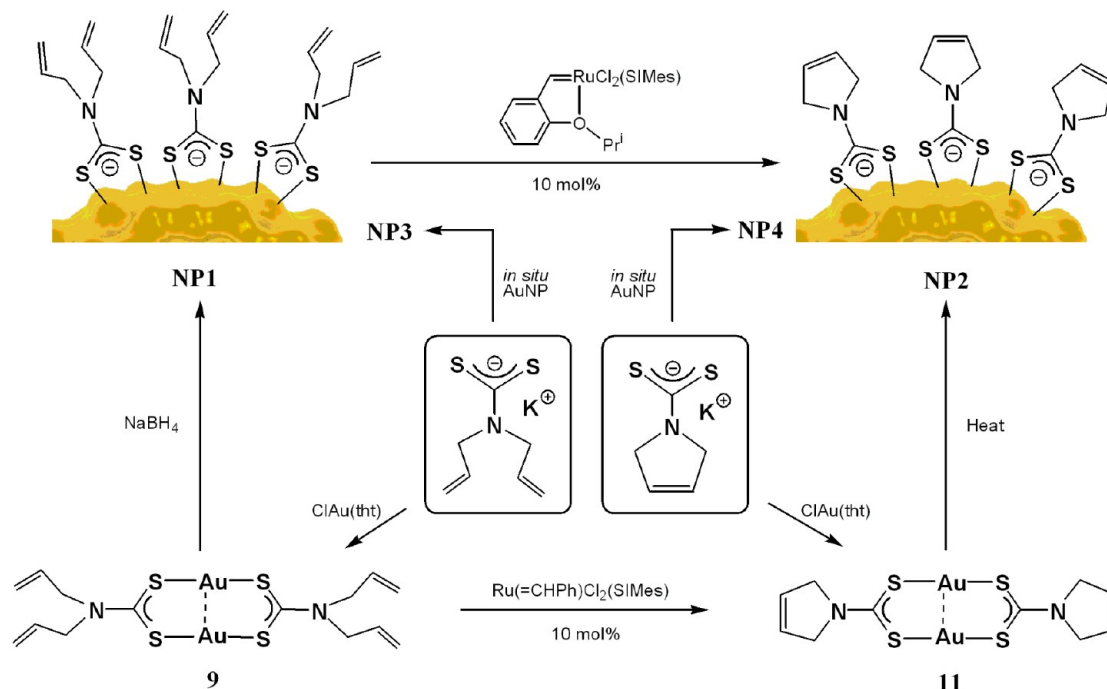
■ STRUCTURAL DISCUSSION

The structural study carried out for complex $[(\text{Ph}_3\text{P})\text{Au}\{\text{S}_2\text{CN}(\text{CH}_2\text{CH}=\text{CH}_2)_2\}]$ (**1**) reveals the expected linear geometry at the gold(I) center [174.980(16) Å]. The bonding mode of the diallyldithiocarbamate ligand is best described as anisobidentate, with the Au–S(1) length of 2.3456(4) Å being much shorter than the distance between the gold and the other sulfur donor [S(3)], which is 3.0020(5) Å. The sum of the van der Waals radii for gold and sulfur is 3.46 Å.¹⁴ The difference in the S(1)–C(2) and C(2)–S(3) distances is significant at 1.7436(17) and 1.6971(17) Å, respectively, indicating substantial multiple bond character in the non-coordinating arm of the dithiocarbamate ligand. The C(2)–N(4) length of 1.341(2) Å suggests modest multiple bond character. The other bond lengths of the 1,1-dithio ligand are unremarkable.

In contrast to compound **1**, the dithiocarbamate ligands are coordinated in a bridging fashion in the structure of the metallacyclic complex $[\text{Au}_2\{\text{S}_2\text{CN}(\text{CH}_2\text{CH}=\text{CH}_2)_2\}_2]$ (**9**). The bonding patterns of the two unique dithiocarbamate ligands are very similar, the Au–S and S–C bond lengths and the S–C–S angles all being nearly identical, with the symmetric C–S bond lengths indicating evenly distributed multiple bond character in the CS_2 units, in contrast to compound **1**. The contribution of the thioureide $[\text{R}_2\text{N}^+=\text{C}(\text{S})_2^-]$ resonance form is observable in the C(2)–N(4) and C(12)–N(14) distances of 1.338(4) and 1.330(4) Å, respectively.

In such metallacycles, it is common to detect the contribution of aurophilic interactions in the short intramolecular Au...Au distances observed.¹⁵ In complex **9**, a very

Scheme 2. SIMes = 1,3-bis(2,4,6-trimethylphenyl)imidazolidin-2-ylidene; tht = tetrahydrothiophene



short Au(1)⋯Au(2) distance of 2.79030(15) Å is observed. This is shorter than the distance of 2.9617(7) Å found in $[\text{Au}_2\{\text{S}_2\text{CN}(\text{C}_5\text{H}_{11})_2\}_2]$ ¹⁶ and substantially below the sum of the van der Waals radii of 3.32 Å.¹⁴ Although the S–Au–S angles are both very close to linear [176.41(3) and 177.10(3)°], on closer inspection, it can be seen that the gold(I) centers deviate slightly toward each other, showing that their close proximity is not solely due to the requirements of the bridging ligands. In addition to these intramolecular interactions, surprisingly short intermolecular contacts of 2.98997(15) Å are also observed (Figure 4). This is only slightly longer than the 2.9617(7) Å found in $[\text{Au}_2\{\text{S}_2\text{CN}(\text{C}_5\text{H}_{11})_2\}_2]$, and a search of the crystallographic literature reveals that the distance in **9** is among the shortest 20% of intermolecular distances observed between gold(I) centers.¹⁷

Given that compound **9** forms gold nanoparticles on reduction with sodium borohydride, it is attractive to imagine that the aurophilic contacts present in the precursor may influence the formation of nanoparticles. This pathway has been implicated in investigations by Xia and co-workers.¹⁸

Ring-Closing Metathesis Experiments. In previous work, inspired by the research of Gladysz and co-workers,¹⁹ we demonstrated for the first time that coordinated dithiocarbamate ligands could be ring-closed even in sterically encumbered environments.⁹ The linear geometry of gold(I) compounds should render them open to the approach of the active species generated from the Grubbs second-generation metathesis catalyst, $[\text{Ru}(\text{=CHPh})\text{Cl}_2(\text{SIMes})(\text{PCy}_3)]$ (SIMes = 1,3-bis(2,4,6-trimethylphenyl)imidazolidin-2-ylidene). However, after stirring $[(\text{Ph}_3\text{P})\text{Au}\{\text{S}_2\text{CN}(\text{CH}_2\text{CH}=\text{CH}_2)_2\}]$ (**1**) for hours and then days under nitrogen, the gold complex was recovered unchanged. To ascertain whether there was some inherent instability in the ring-closed product $[(\text{Ph}_3\text{P})\text{Au}(\text{S}_2\text{CNC}_4\text{H}_6)]$ (**10**), this was prepared directly from a solution of 3-pyrrolinedithiocarbamate (Scheme 1). ¹H NMR analysis revealed singlet resonances at 4.49 (NCH₂) and 5.96 ppm (CH=CH) in addition to peaks in the aromatic region for the

coordinated triphenylphosphine, which were very similar to those found for $[\text{Ni}(\text{S}_2\text{CNC}_4\text{H}_6)_2]$.⁹ Mass spectrometry and elemental analysis data were also in agreement with the formulation. Having established that the product was viable, our attention returned to the RCM reaction. It was a possibility that the PPh₃ unit could be liberated from **1** and coordinate to the catalyst, causing deactivation— $[\text{Ru}(\text{=CHPh})\text{Cl}_2(\text{SIMes})(\text{PPh}_3)]$ is known to be far less active. However, no ring-closed product was observed with the tricyclohexylphosphine complex $[(\text{Cy}_3\text{P})\text{Au}\{\text{S}_2\text{CN}(\text{CH}_2\text{CH}=\text{CH}_2)_2\}]$ (**2**) either. Eliminating phosphines from the gold substrate entirely with $[(^t\text{BuNC})\text{Au}\{\text{S}_2\text{CN}(\text{CH}_2\text{CH}=\text{CH}_2)_2\}]$ (**4**) had no beneficial effect, but did result in deposition of gold metal on the glassware (even under nitrogen).

It appeared that complex **1** was having a deactivating effect on the catalyst. The RCM of $[\text{Ni}\{\text{S}_2\text{CN}(\text{CH}_2\text{CH}=\text{CH}_2)_2\}]$ to $[\text{Ni}(\text{S}_2\text{CNC}_4\text{H}_6)_2]$ using 10 mol % $[\text{Ru}(\text{=CHPh})\text{Cl}_2(\text{SIMes})(\text{PCy}_3)]$ was used to test this hypothesis. This reaction proceeds within an hour at room temperature in dichloromethane.^{9a} To explore the deactivating effect of **1**, an equimolar amount of this gold complex was added (under N₂) to the dichloromethane solution of the Grubbs precatalyst (10 mol % loading). $[\text{Ni}\{\text{S}_2\text{CN}(\text{CH}_2\text{CH}=\text{CH}_2)_2\}]$ was then introduced, and the reaction was stirred and monitored by ³¹P NMR. After 1 h, gold complex **1** was no longer observed, but instead two new resonances at 54.9 (major) and 42.4 ppm (minor) were observed (as well as some of the original Grubbs precatalyst at 28.8 ppm). In the ¹H NMR spectrum, only 8% conversion to the ring-closed nickel product was observed. After 3 d, 58% conversion had been achieved, which thereafter remained unchanged. After 4 d a new, yet significant, peak was seen in the ³¹P NMR spectrum at 25.0 ppm. In the conventional RCM reaction of $[\text{Ni}\{\text{S}_2\text{CN}(\text{CH}_2\text{CH}=\text{CH}_2)_2\}]$ without any gold complex, the only resonances in the ³¹P NMR spectrum were at 28.8 (Grubbs precatalyst) and 22.5 (putatively a solvent-stabilized catalyst species) ppm. Therefore, it seems that an adduct was formed during the reaction

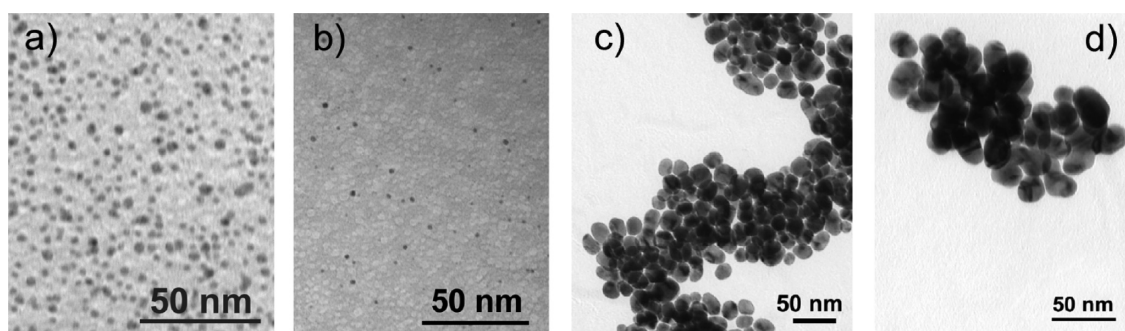


Figure 5. Au@S₂CN(CH₂CH=CH₂)₂ (NP1, a) and Au@S₂CNC₄H₆ (NP2, b) nanoparticles prepared directly and Au@S₂CN(CH₂CH=CH₂)₂ (NP3, c) and Au@S₂CNC₄H₆ (NP4, d) nanoparticles prepared via a citrate-stabilized intermediate.

between [Ru(=CHPh)Cl₂(SIMes)(PCy₃)] and [(Ph₃P)Au{S₂CN(CH₂CH=CH₂)₂}] (1), which gave rise to a peak at 54.9 ppm (negligible PCy₃ or O=PCy₃ were observed in the spectra). The compound responsible for this peak did not prove amenable to isolation using polar or non-polar antisolvents and could not be identified further.

While all the diallyldithiocarbamate complexes of groups 8–10 investigated in RCM displayed bidentate coordination of the 1,1-dithio ligand,⁹ the monodentate (or anisobidentate) mode is adopted in complexes 1–5, which do not undergo RCM. Thus, preferential coordination of a lone pair on the pendant sulfur to the vacant site at the ruthenium center could lead to deactivation of the catalyst toward alkenes. To test this, [Au₂{S₂CN(CH₂CH=CH₂)₂}] (9), in which both sulfurs are coordinated, was treated with 10 mol % [Ru(=CHPh)Cl₂(SIMes)(PCy₃)] in dichloromethane under nitrogen. After 2 h, analysis of the product revealed no resonances for 9. Instead, two new peaks were observed at 4.52 and 6.00 ppm, corresponding to the NCH₂ and CH=CH protons of the ring-closed product [Au₂(S₂CNC₄H₆)₂] (11). The nature of this product (Scheme 1) was confirmed by mass spectrometry (ES +ve mode) and elemental analysis. Furthermore, 11 was also prepared directly from [(tht)AuCl] and 3-pyrrolinedithiocarbamate.

Preparation of Gold Nanoparticles. The reduction of well-defined gold(I) precursors containing phosphine,²⁰ amine,^{18,21} alkyl,²² carboxylate,²³ and, most recently, carbene²⁴ ligands has been shown to yield ligand-stabilized gold nanoparticles. Direct routes to thiolate-capped gold nanoparticles have also been reported from gold(I) thiolate precursors, which are often polymeric or cyclic in nature.^{25a–25c}

This approach has been extended to patterning using e-beam lithography/thermolysis protocols.^{25d,e} Recently, the thermal preparation (140 °C) of thiol-coated gold nanoparticles was reported from molecular methylgold(I) precursors in the presence of thiol surfactants.²² In contrast, thermolysis of monometallic dithiolate complexes has been shown to afford gold nanoparticles stabilized by alkyl groups.²⁶ Along with others,¹² we have demonstrated^{18a–c} that dithiocarbamate ligands make excellent surface units for gold nanoparticles.²⁷ Accordingly, it was decided to explore whether direct preparation of nanoparticles from [Au₂{S₂CN(CH₂CH=CH₂)₂}] (9) was possible, using sodium borohydride as the reducing agent. On addition of this reagent to an acetone solution of 9, an immediate darkening occurred, leading to precipitation of a black solid (Scheme 2). After purification, this material was analyzed by solid-state infrared spectroscopy to show absorptions similar to those for the dithiocarbamate

ligand in the precursor. The ¹H NMR spectrum revealed resonances characteristic of the diallyldithiocarbamate ligand at 4.06, 4.94, 4.99, and 5.53 ppm, shifted from the positions found in 9. Transmission electron microscopy (TEM) showed nanoparticles (Figure 5a) of Au@S₂CN(CH₂CH=CH₂)₂ (NP1) of diameter 4.8 (±0.7) nm. The size distribution is similar to that found for our earlier preparation of dithiocarbamate-protected nanoparticles, using the Brust-Schiffrin method (in situ reduction of gold(III) in the presence of a phase-transfer agent and sulfur ligand).

It was found that a solution of [Au₂(S₂CNC₄H₆)₂] (11), formed by ring-closing of 9, spontaneously converted to gold nanoparticles on gentle warming. The process was complete after 30 min, and analysis of the black material by IR and ¹H NMR spectroscopy revealed it to be Au@S₂CNC₄H₆ (NP2). The TEM image of this material (Figure 5b) showed dispersed nanoparticles of diameter 4.0 (±0.7) nm.

The citrate reduction of HAuCl₄ is a well-known method, pioneered by Turkevich, used to prepare nanoparticles of around 15–20 nm diameter.²⁸ In earlier work, we have demonstrated that the citrate shell can be successfully displaced by dithiocarbamate units prepared in situ.^{8a–c} Using this approach, Au@S₂CN(CH₂CH=CH₂)₂ (NP3) nanoparticles of 13.7 (±3.6) nm were prepared (Figure 5c). After repeated washing with water to remove uncoordinated dithiocarbamate, analysis by infrared and ¹H NMR spectroscopy revealed the presence of the diallyldithiocarbamate surface units. TEM imaging showed a surprisingly large size distribution. Using the same citrate reduction approach, Au@S₂CNC₄H₆ (NP4) nanoparticles were also prepared (Figure 5d), which showed a much narrower range of diameters (15.0 ± 1.8 nm). Again, the presence of the 3-pyrroline-dithiocarbamate surface units was confirmed by ¹H NMR and IR spectroscopies.

Under similar conditions, heating 1 or 2 (or treating with NaBH₄) only led to deposition of gold metal rather than facile formation of nanoparticles. This suggests that there is an advantage possessed by the metallacyclic compounds (9 and 11) in this process. It is tempting to imagine that the existence of the Au₂(S₂CNR₂)₂ metallacycle provides a degree of preorganization, which favors the formation of the nanoparticle material. This phenomenon has been postulated to play a role in the formation of gold nanowires from [(oleylamine)AuCl] complexes.^{21a}

In a similar way in which the fate of the thiol proton is unclear in many thiol/thiolate-capped gold nanoparticles,²⁹ the nature of the interaction between the dithiocarbamate and the gold surface has not been elucidated in detail. Energy dispersive X-ray (EDX) spectroscopic analysis failed to reveal the

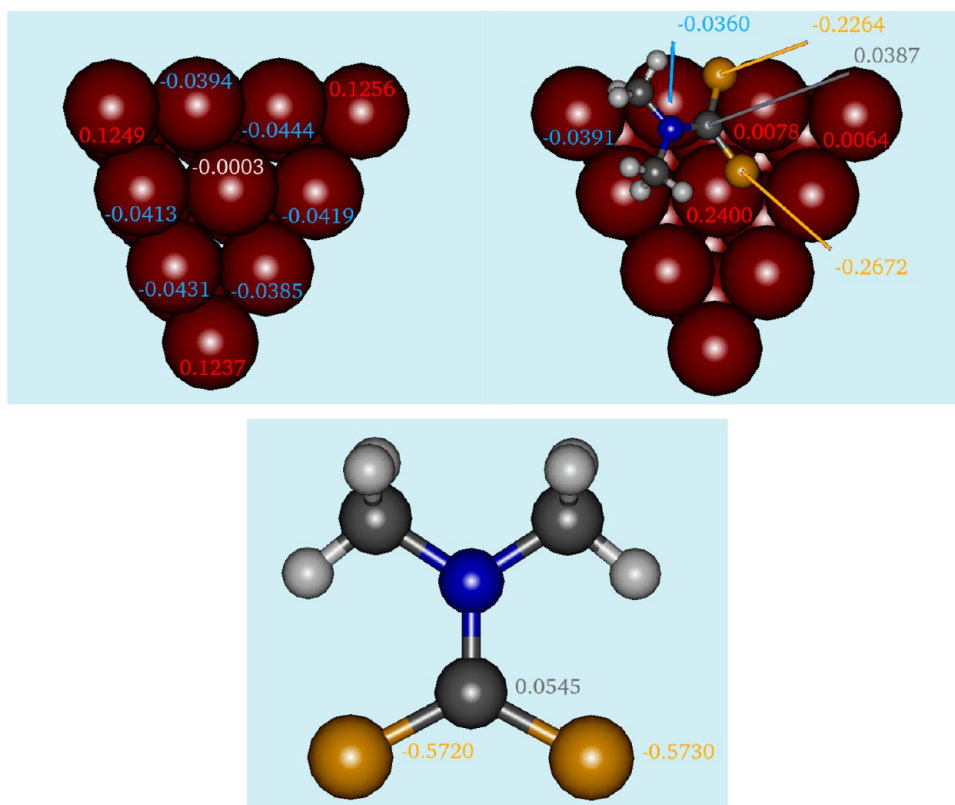


Figure 6. Charge on key atoms of optimized (top left) Au_{20} , (below) $\text{Me}_2\text{NCS}_2^-$, and (top right) face-adsorbed $\text{Au}_{20}(\text{S}_2\text{CNMe}_2)^-$. Atoms: brown: Au; gray: C; white: H; yellow: S; blue: N. Charge numbers: white: near-neutral Au; red: positive Au; blue: negative Au; yellow: S; gray: C.

presence of sodium (NP1) or potassium ions (NP3, NP4) acting as counterions for the anionic dithiocarbamate. NP2 was obtained directly and spontaneously from heating the $[\text{Au}_2(\text{S}_2\text{CNC}_4\text{H}_6)_2]$ (11) precursor in the absence of sodium borohydride. In this case, it was initially postulated that electroneutrality in this material could be provided by $[\text{H}_2\text{N}(\text{C}_4\text{H}_6)]^+$ cations formed from the decomposition of excess surface units; however, no evidence for these units (e.g., IR, ^1H NMR spectroscopy) was found. This observation prompted our theoretical investigations (outlined in the Computational Section), which suggested electronic charge is partly transferred to and dispersed throughout the gold nanocluster, thus obviating the need for a balancing counterion. Also, complete removal of the -1 charge was found to be energetically more favorable in presence of the dithiocarbamate.

Once nanoparticles of different sizes bearing both $[\text{S}_2\text{CN}(\text{CH}_2\text{CH}=\text{CH}_2)_2]^-$ and $[\text{S}_2\text{CNC}_4\text{H}_6]^-$ surface units had been prepared, investigations took place to attempt to ring-close nanoparticles NP3 to generate NP4. The approximate coverage of the nanoparticles with the surface units was calculated based on a 70% coverage using a “footprint” of the ligand drawn from the crystal structure of compound 9. This allowed a rough concentration to be ascertained. The diallyldithiocarbamate-capped nanoparticles (NP3) were stirred for 36 h with a stoichiometric amount of $[\text{Ru}(=\text{CHPh})\text{Cl}_2(\text{SIMes})(\text{PCy}_3)]^{30}$ under nitrogen; however, no reaction was apparent. Repeating the reaction with the Grubbs–Hoveyda catalyst $[\text{Ru}(=\text{CHC}_6\text{H}_4\text{O}^i\text{Pr}-2)\text{Cl}_2(\text{SIMes})]^{31}$ under the same conditions led to successful generation of NP4 (Scheme 2) in effectively quantitative yield (^1H NMR). This phosphine-free catalyst is known to tolerate many functional groups that would

deactivate $[\text{Ru}(=\text{CHPh})\text{Cl}_2(\text{SIMes})(\text{PCy}_3)]^{32}$ and this aspect may be the deciding factor in the differing course of this reaction. This result illustrates that RCM can be achieved both in molecular and in nanoparticulate assemblies of the diallyldithiocarbamate ligand. By extension of this approach, further in situ functionalization of the nanoparticle surface architecture could be achieved through cross metathesis of suitable surface units, for example, $\text{Au}@_2\text{CN}(\text{Me})\text{CH}_2\text{CH}=\text{CH}_2$.

Computational Section. Substantial efforts have been concentrated on elucidating the nature of the interaction between thiols/thiolates and the surface of gold nanoparticles.^{29a,33,34} Two key aspects which have been probed successfully are the formally homolytic cleavage of the S–H bond on addition of thiols to a nanoparticle surface^{29b,35–38} and the disruption of the gold surface on attachment of the sulfur unit. In the latter case, $[\text{RS–Au–SR}]$ and $[\text{RS–Au–S(R)–Au–SR}]$ “staples” have been observed in systems probed both crystallographically^{39–42} and theoretically.^{43,44} In these reports, one or two gold atoms are shown to be lifted from the crystallographic plane and pinned between RS^- units. In contrast to the efforts expended on computational studies of thiolate-coated nanoparticle systems, very little is known about their dithiocarbamate-covered counterparts.

As a result of this, a series of explorative density functional theory (DFT) computations were carried out. Our initial focus was to investigate the lack of counterion observed in the experimental data discussed above. To this purpose, properties of pristine Au_{20} and Au_{20}^+ nanoclusters were investigated and compared to those of face-adsorbed $\text{Au}_{20}(\text{S}_2\text{CNMe}_2)^-$ (consisting of formally zerovalent gold atoms), face-adsorbed $\text{Au}_{20}(\text{S}_2\text{CNMe}_2)$ (consisting of one

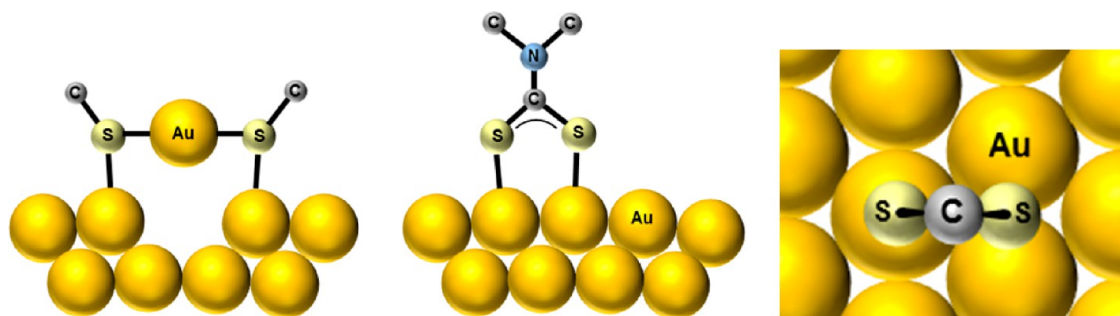


Figure 7. The extensive reconstruction upon thiol self-assembly (with formation of [RS–Au–SR] staples on the left) contrasts with the almost unaffected surface seen upon dithiocarbamate adsorption (center and plan view on the right).

formally monovalent and 19 formally zerovalent gold atoms), and unbound $\text{Me}_2\text{NCS}_2^-$. In addition to its convenient size in terms of computational efficiency, pristine Au_{20} is known experimentally^{45,46} and computationally^{45–49} to feature a highly stable tetrahedral isomer (T_d) with four Au(111) faces analogous to those recognized in larger pristine nanoparticles.⁵⁰ Dimethyldithiocarbamate ($\text{Me}_2\text{NCS}_2^-$) was chosen to replace the diallyldithiocarbamate, given the smaller size of the former.

Analysis of charge distribution in pristine Au_{20} (Figure 6) shows depletion at each of the four vertex atoms (average: +0.125) and accumulation at each of the 12 central edge atoms (average: –0.042), with the four atoms at the center of each face remaining close to neutrality. Comparison of this with the distribution in $\text{Au}_{20}(\text{S}_2\text{CNMe}_2)^-$ and $\text{Me}_2\text{NCS}_2^-$ (Figure 6) clearly reveals that, upon dithiocarbamate adsorption, a partial charge transfer from ligand to nanocluster occurs. The loss of electronic charge is evident when comparing sulfur charges in the free and bound ligand. Furthermore, our values predict that the charge depletion extends to the one center-face and two center-edge gold atoms bonded to the sulfur: the transferred charge accumulates *away* from the adsorption site, on the vertex gold atoms.

Our calculations also revealed that adsorption of a single dimethyldithiocarbamate ligand on one of the Au_{20} faces is enough to significantly lower the ionization potential (IP) from the 7.31 eV (vertical)/7.28 eV (adiabatic) required for the conversion $\text{Au}_{20} \rightarrow \text{Au}_{20}^+$ to as little as the 3.61 eV (vertical)/3.34 eV (adiabatic) required for $\text{Au}_{20}(\text{S}_2\text{CNMe}_2)^- \rightarrow \text{Au}_{20}(\text{S}_2\text{CNMe}_2)$. Thus, the complete removal of one electron, equivalent to removing the –1 charge in $\text{Au}_{20}(\text{S}_2\text{CNMe}_2)^-$, is greatly facilitated. Applying the findings described above to the diallyldithiocarbamate system studied here obviates the need for sodium, potassium, or other countercations to balance the charge of the anionic surface unit. The absence of these cations in the EDX data supports this theoretical observation.

The discovery that stapling occurs in thiolate-gold systems (Figure 7) has caused researchers to depart from the view of simple chemisorption of such sulfur units at regular sites on the surface of gold nanoparticles. In the absence of thiols, raising one gold atom out of the surface comes at a significant energetic cost, quantified by us at 1.95 eV for pristine tetrahedral Au_{20} . However, when two methanethiyl radicals ($\cdot\text{SCH}_3$) are adsorbed on (frozen) Au_{20} and the $\text{Au}_{20}(\text{SCH}_3)_2$ system is allowed to relax, staple formation is spontaneous, affording an energetic *gain* of 0.97 eV with respect to unstapled $\text{Au}_{20}(\text{SCH}_3)_2$. This is a contributing factor to the stability of the monolayers obtained. We calculate that the total energy change upon adsorption of two $\cdot\text{SCH}_3$ units on T_d Au_{20} *along with* staple formation is –3.55 eV. Adsorption on Au_{20} that has

already been reconstructed is even more favorable (–5.50 eV). By comparison, Jiang et al. report –6.88 eV for the first staple of Au_{38} and –4.44 eV for a staple on a Au(111) surface.⁴³ Also, Askarka et al.^{44b} have recently conducted a full mechanistic DFT study, in which they explore reaction pathways when two methanethiol molecules (HSCH_3) are adsorbed on T_d Au_{20} : staple formation *and* evolution of H_2 are achieved via a series of intermediate structures. The calculated net energy gain for this reaction, which comprises the cost of cleaving two S–H bonds and forming one H–H bond, is 1.86 eV.

When performing the calculations with $\text{Au}_{20}(\text{S}_2\text{CNMe}_2)^-$ and $\text{Au}_{20}(\text{S}_2\text{CNMe}_2)$ discussed above, we observe radically different results compared to those obtained for methanethiyl adsorption. The carbon and sulfur atoms of the dithiocarbamate merely undergo a slight out-of-plane displacement (Figure 7), and reconstruction is very limited compared to staple formation. This lack of disruption of the gold surface would change the energetics of monolayer formation substantially and may help to explain the observation^{12b,f,g} that dithiocarbamate units are often less easily lost from the gold surface than comparable thiolate units. For example, our preliminary calculations predict an energy change of –0.32 eV for the process of $\text{Au}_{20}(\text{SCH}_3)_2 + \text{Me}_2\text{NCS}_2^- \rightarrow \text{Au}_{20}(\text{S}_2\text{CNMe}_2)^- + 2\text{H}_3\text{CS}\cdot$ when Au_{20} is kept frozen in the T_d geometry. Similarly, the hypothetical process $\text{Au}_{20}(\text{SCH}_3)_2 + \text{Me}_2\text{NCS}_2^- \rightarrow \text{Au}_{19}(\text{S}_2\text{CNMe}_2)^- + \text{H}_3\text{CS–Au–SCH}_3$ (*trans*), where the dithiocarbamate replaces a whole neutral staple unit (all species fully optimized), affords a gain in energy of 0.28 eV.

These preliminary results demonstrate that dithiocarbamate–gold nanoparticle systems behave very differently to thiolate–gold systems, dispelling the suggestion that dithiocarbamates are simply a disulfur version of conventional thiolate surface units. Additional investigations from our computational studies will be presented in more detail in the near future.

■ SUMMARY AND CONCLUSION

The potential for straightforward modification of ligand architecture within the coordination sphere of a metal using RCM has been demonstrated using metallacyclic gold(I) dithiocarbamate complexes. However, the issues which arise from substrates with available electron pairs are also demonstrated in the compounds bearing dithiocarbamate ligands in monodentate or anisobidentate coordination modes.

For the first time, molecular dithiocarbamate precursors have been used to directly generate functionalized gold nanoparticles. In one case, simple heating is sufficient to generate these materials with a narrow size distribution. The use of

gold(I) precursors, rather than trivalent species, renders the process more facile (c.f. the standard reduction potentials for Au^+/Au and $\text{Au}^{3+}/\text{Au}^{2\text{b}}$) and requires only a single-electron reduction per gold center. It has also been demonstrated that RCM of these surface units can be achieved successfully. Future work will extend the potential of metathesis and other transformations to create more complex architectures from similar dithiocarbamate ligands both in molecular and nanoparticulate assemblies (e.g., through cross metathesis).

The preliminary computations reported here reveal that upon adsorption dithiocarbamates transfer and disperse part of the charge across the nanocluster. Charge depletion is seen to occur in atoms interacting directly with the ligand, whereas a slight accumulation of charge is observed on outlying gold atoms. We also observe that dithiocarbamate adsorption on a nanocluster facilitates its overall oxidation. Furthermore, the behavior of the dithiocarbamate surface unit at the gold surface is significantly different than that observed with thiolates, in that no stapling is observed and little rearrangement appears to be necessary after their adsorption.

EXPERIMENTAL SECTION

General Comments. Unless otherwise stated, all experiments were carried out in air, and the complexes obtained appear stable toward the atmosphere, whether in solution or in the solid state. Reagents and solvents were used as received from commercial sources. Petroleum ether is the fraction boiling in the 40–60 °C range. The following complexes were prepared as described elsewhere: $[\text{AuCl}(\text{PR}_3)]$, ($\text{R} = \text{Me}$,⁵¹ Cy ,⁵² Ph^{53}), $[\text{dppf}(\text{AuCl})_2]$ (1,1'-bis-(diphenylphosphino)ferrocene),⁵⁴ $[\text{dppm}(\text{AuCl})_2]$ (1,1-bis-(diphenylphosphino)methane),⁵⁵ $[\text{dppa}(\text{AuCl})_2]$ (1,2-bis-(diphenylphosphino)acetylene),⁵³ $[\text{AuCl}(\text{tht})]$,⁵⁶ $[\text{AuCl}(\text{CN}^t\text{Bu})]$,⁵⁷ $[\text{AuCl}(\text{IDip})]$ (IDip = 1,3-bis(2,6-diisopropylphenyl)imidazol-2-ylidene),⁵⁸ $[\text{Ru}(\text{=CHPh})\text{Cl}_2(\text{SIMes})(\text{PCy}_3)]$ (SIMes = 1,3-bis(2,4,6-trimethylphenyl)imidazol-2-ylidene),³⁰ and $[\text{Ru}(\text{=CHC}_6\text{H}_4\text{O}^i\text{Pr}-2)\text{Cl}_2(\text{SIMes})]$.³¹ Electrospray (ES) and fast atom bombardment (FAB) mass data were obtained using Micromass LCT Premier and Autospec Q instruments, respectively. Infrared data were obtained using a Perkin-Elmer Spectrum 100 FT-IR spectrometer, and characteristic triphenylphosphine-associated infrared data are not reported. NMR spectroscopy was performed at 25 °C using Varian Mercury 300 and Bruker AV400 spectrometers. All coupling constants are in Hertz. Resonances in the ³¹P NMR spectrum due to the hexafluorophosphate counteranion were observed in all cases but are not included below. Elemental analysis data were obtained from London Metropolitan University. The procedures given provide materials of sufficient purity for synthetic and spectroscopic purposes. Initial TEM measurements were performed at University College London using a JEOL 100 instrument operating at 100 kV. Further TEM images and EDX data were obtained at Imperial College using a JEOL 2010 high-resolution TEM (80–200 kV) equipped with an Oxford Instruments INCA EDS 80 mm X-Max detector system.

$\text{KS}_2\text{CN}(\text{CH}_2\text{CH}=\text{CH}_2)_2$. Diallylamine (1.00 mL, 8.100 mmol) and CS_2 (0.59 mL, 9.810 mmol) were stirred in the presence of KOH (500 mg, 8.933 mmol) in water (40 mL) for 40 min. Assuming complete conversion, this solution was used (in slight excess) for the subsequent additions to the metal precursors.⁹

$\text{KS}_2\text{CNC}_4\text{H}_6$. An aqueous solution (30 mL) of 3-pyrroline (34.8 μL , 0.458 mmol) and KOH (32.5 mg, 0.579 mmol) was stirred for 10 min and then treated with carbon disulfide (41.7 μL , 52.8 mg, 0.693 mmol). After stirring for a further 40 min, complete conversion was assumed, and this solution was used (in slight excess) for the subsequent additions to the metal precursors.⁹

$[(\text{Ph}_3\text{P})\text{Au}\{\text{S}_2\text{CN}(\text{CH}_2\text{CH}=\text{CH}_2)_2\}]$ (1). A solution of $[\text{AuCl}(\text{PPh}_3)]$ (300 mg, 0.605 mmol) in acetone (20 mL) and dichloromethane (10 mL) was treated with 1.1 equiv of $\text{KS}_2\text{CN}(\text{CH}_2\text{CH}=\text{CH}_2)_2$ in water (3.41 mL), and the reaction stirred for 30 min. All solvent was

removed, and the residue was dissolved in the minimum volume of dichloromethane and filtered through diatomaceous earth (Celite) to remove KCl and excess ligand. All solvent was again removed; petroleum ether (30 mL) was added, and the solid was triturated ultrasonically. The yellow product was washed with water (10 mL) and petroleum ether (10 mL) and dried under vacuum. Yield: 369 mg (77%). IR (solid state): 1644, 1467, 1399, 1354, 1277, 1221, 1174, 978, 943, 906 cm^{-1} ; ³¹P NMR: δ 36.3 (s, PPh_3) ppm; ¹H NMR: δ 4.59 (m, 4 H; NCH_2), 5.25 (m, 4 H; $=\text{CH}^{\text{A,B}}$), 5.98 (m, 2 H; $=\text{CH}^{\text{C}}$), 7.44–7.53, 7.61–7.67 (m \times 2, 15 H; C_6H_5) ppm; ¹³C NMR (CD_2Cl_2 , 400 MHz): δ 209.0 (s, CS_2), 134.5 (d, $J_{\text{CP}} = 13.9$ Hz; $o/m\text{-PC}_6\text{H}_5$), 132.2 (s, $=\text{CH}_2$), 131.8 (d, $J_{\text{CP}} = 1.7$ Hz; $p\text{-PC}_6\text{H}_5$), 130.7 (d, $J_{\text{CP}} = 56.8$ Hz; $ipso\text{-PC}_6\text{H}_5$), 129.4 (d, $J_{\text{CP}} = 11.3$ Hz; $o/m\text{-PC}_6\text{H}_5$), 118.0 (s, CH_2C), 56.4 (s, NCH_2) ppm; MS (ES +ve) m/z (%) 632 (22) [M^+]; Anal. Calcd (%) for $\text{C}_{25}\text{H}_{25}\text{AuNPS}_2$ ($M_w = 631.55$): C 47.6, H 4.0, N 2.2. Found: C 47.6, H 4.1, N 2.3.

$[(\text{Cy}_3\text{P})\text{Au}\{\text{S}_2\text{CN}(\text{CH}_2\text{CH}=\text{CH}_2)_2\}]$ (2). A solution of $[\text{AuCl}(\text{PCy}_3)]$ (60 mg, 0.117 mmol) in dichloromethane (10 mL) and methanol (5 mL) was treated with 1.1 equiv of $\text{KS}_2\text{CN}(\text{CH}_2\text{CH}=\text{CH}_2)_2$ in water (0.66 mL), and the reaction was stirred for 1 h. All solvent was removed, and the residue was dissolved in the minimum volume of dichloromethane and filtered through diatomaceous earth (Celite) to remove KCl and excess ligand. All solvent was again removed; diethyl ether (20 mL) was added, and the solid was triturated ultrasonically. The bright yellow product was washed with petroleum ether (10 mL) and dried under vacuum. Yield: 55 mg (72%). IR (solid state): 2921, 2850, 1740, 1641, 1466, 1447, 1423, 1390, 1331, 1278, 1222, 1175, 1114, 996, 972, 932, 852, 820 cm^{-1} ; ³¹P NMR (acetone- d_6): δ 56.0 (s, PCy_3) ppm; ¹H NMR (acetone- d_6): δ 1.25–1.88, 2.20 (m \times 2, 30 H + 3 H; PCy_3), 4.54 (d, $J_{\text{HH}} = 5.8$ Hz, 4 H; NCH_2), 5.22 (dd, $J_{\text{HHBC}} = 8.8$ Hz, $J_{\text{HBHA}} = 1.4$ Hz, 2 H; $=\text{CH}^{\text{B}}$), 5.25 (dd, $J_{\text{HAHC}} = 15.9$ Hz, $J_{\text{HAHB}} = 1.4$ Hz, 2 H; $=\text{CH}^{\text{A}}$), 5.97 (m, 2 H; $=\text{CH}^{\text{C}}$) ppm; MS (FAB +ve) m/z (%) 650 (53) [M^+]; Anal. Calcd (%) for $\text{C}_{25}\text{H}_{43}\text{AuNPS}_2$ ($M_w = 649.69$): C 46.2, H 6.7, N 2.2. Found: C 46.0, H 6.8, N 2.1.

$[(\text{Me}_3\text{P})\text{Au}\{\text{S}_2\text{CN}(\text{CH}_2\text{CH}=\text{CH}_2)_2\}]$ (3). A solution of $[\text{AuCl}(\text{PMe}_3)]$ (40 mg, 0.130 mmol) in dichloromethane (10 mL) and methanol (5 mL) was treated with 1.1 equiv of $\text{KS}_2\text{CN}(\text{CH}_2\text{CH}=\text{CH}_2)_2$ in water (0.73 mL), and the reaction was stirred for 1 h. All solvent was removed, and the residue was dissolved in the minimum volume of dichloromethane and filtered through diatomaceous earth (Celite) to remove KCl and excess ligand. All solvent was again removed, and the oil was triturated ultrasonically with ethanol (20 mL). The bright yellow product was washed with petroleum ether (10 mL) and dried under vacuum. Low yield is due to high solubility in ethanol. Yield: 37 mg (64%). IR (solid state): 1640, 1461, 1416, 1392, 1334, 1280, 1222, 1171, 1123, 1065, 942, 925, 858 cm^{-1} ; ³¹P NMR (acetone- d_6): δ -6.3 (s, PMe_3) ppm; ¹H NMR (acetone- d_6): δ 1.65 (d, $J_{\text{HP}} = 11.0$ Hz, 9 H; PMe_3), 4.54 (d, $J_{\text{HH}} = 5.7$ Hz, 4 H; NCH_2), 5.19 (dd, $J_{\text{HHBC}} = 10.1$ Hz, $J_{\text{HBHA}} = 1.4$ Hz, 2 H; $=\text{CH}^{\text{B}}$), 5.21 (dd, $J_{\text{HAHC}} = 17.2$ Hz, $J_{\text{HAHB}} = 1.4$ Hz, 2 H; $=\text{CH}^{\text{A}}$), 5.94 (m, 2 H; $=\text{CH}^{\text{C}}$) ppm; MS (FAB +ve) m/z (%) 446 (42) [M^+]; Anal. Calcd (%) for $\text{C}_{10}\text{H}_{19}\text{AuNPS}_2$ ($M_w = 445.37$): C 27.0, H 4.3, N 3.2. Found: C 27.1, H 4.2, N 3.1.

$[(^t\text{BuNC})\text{Au}\{\text{S}_2\text{CN}(\text{CH}_2\text{CH}=\text{CH}_2)_2\}]$ (4). A solution of $[\text{AuCl}(\text{CN}^t\text{Bu})]$ (60 mg, 0.190 mmol) in dichloromethane (10 mL) and methanol (5 mL) was treated with 1.1 equiv of $\text{KS}_2\text{CN}(\text{CH}_2\text{CH}=\text{CH}_2)_2$ in water (1.07 mL), and the reaction was stirred for 0.5 h. All solvent was removed, and the solid residue was triturated ultrasonically with diethyl ether (20 mL) and filtered. The yellow product was washed with water (10 mL), cold ethanol (5 mL), and petroleum ether (10 mL) and dried under vacuum. Yield: 62 mg (72%). IR (solid state): 3083, 2984, 2203 (ν_{CN}), 1641, 1469, 1397, 1344, 1329, 1269, 1219, 1163, 1121, 970, 933, 906 cm^{-1} ; ¹H NMR (benzene- d_6): δ 0.53 (s, 9 H; ^tBu), 4.15 (d, $J_{\text{HH}} = 5.7$ Hz, 4 H; NCH_2), 4.90 (dd, $J_{\text{HAHC}} = 17.1$ Hz, $J_{\text{HAHB}} = 1.3$ Hz, 2 H; $=\text{CH}^{\text{A}}$), 4.99 (dd, $J_{\text{HHBC}} = 10.2$ Hz, $J_{\text{HBHA}} = 1.3$ Hz, 2 H; $=\text{CH}^{\text{B}}$), 5.58 (m, 2 H; $=\text{CH}^{\text{C}}$) ppm; MS (FAB +ve) m/z (%) 369 (2) [$\text{M}^+ - ^t\text{BuNC}$]; Anal. Calcd (%) for $\text{C}_{12}\text{H}_{19}\text{AuN}_2\text{S}_2$ ($M_w = 452.39$): C 31.9, H 4.2, N 6.2. Found: C 32.1, 4.5, N 6.4.

$[(\text{IDip})\text{Au}\{\text{S}_2\text{CN}(\text{CH}_2\text{CH}=\text{CH}_2)_2\}]$ (5). A solution of $[\text{AuCl}(\text{IDip})]$ (60 mg, 0.097 mmol) in dichloromethane (10 mL) and acetone (5

mL) was treated with 1.1 equiv of $\text{KS}_2\text{CN}(\text{CH}_2\text{CH}=\text{CH}_2)_2$ in water (0.55 mL), and the reaction was stirred for 1 h. All solvent was removed, and the residue was dissolved in dichloromethane (10 mL) and filtered through diatomaceous earth (Celite) to remove KCl and excess ligand. All solvent was again removed; petroleum ether (20 mL) was added, and the solid was triturated ultrasonically. The yellow product was washed with petroleum ether (10 mL) and dried under vacuum. Yield: 52 mg (70%). IR (solid state): 2960, 2868, 1456, 1387, 1350, 1331, 1277, 1216, 1177, 1108, 1061, 996, 972, 926, 803, 758 cm^{-1} ; ^1H NMR (acetone- d_6): δ 1.25, 1.41 (d \times 2, $J_{\text{HH}} = 6.9$ Hz, 2 \times 12 H; Me_{IDip}), 2.74 (sept, $J_{\text{HH}} = 6.9$ Hz, 4 H; $\text{CHMe}_{\text{IDip}}$), 4.36 (d, $J_{\text{HH}} = 6.9$ Hz, 4 H; NCH_2), 5.08 (dd, $J_{\text{HBHC}} = 7.6$ Hz, J_{HBHA} unresolved, 2 H; $=\text{CH}^{\text{B}}$), 5.09 (dd, $J_{\text{HAHC}} = 17.9$ Hz, J_{HAHB} unresolved, 2 H; $=\text{CH}^{\text{A}}$), 5.80 (m, 2 H; $=\text{CH}^{\text{C}}$), 7.38 (d, $J_{\text{HH}} = 7.8$ Hz, 4 H; $m\text{-C}_6\text{H}_3$), 7.53 (t, $J_{\text{HH}} = 7.8$ Hz, 2 H; $p\text{-C}_6\text{H}_3$), 7.77 (s, 2 H; $\text{HC}=\text{CH}$) ppm; MS (FAB +ve) m/z (%) 758 (23) [M^+]; Anal. Calcd (%) for $\text{C}_{34}\text{H}_{46}\text{AuN}_3\text{S}_2$ ($M_w = 757.85$): C 53.9, H 6.1, N 5.6. Found: C 53.9, H 6.1, N 5.5.

$[(\text{dppa})\{\text{AuS}_2\text{CN}(\text{CH}_2\text{CH}=\text{CH}_2)_2\}_2]$ (**6**). A solution of $[(\text{dppa})\{\text{AuCl}\}_2]$ (60 mg, 0.070 mmol) in dichloromethane (10 mL) and methanol (5 mL) was treated with 2.2 equiv of $\text{KS}_2\text{CN}(\text{CH}_2\text{CH}=\text{CH}_2)_2$ in water (0.79 mL), and the reaction was stirred for 1 h. All solvent was removed, and the residue was dissolved in the minimum volume of dichloromethane and filtered through diatomaceous earth (Celite) to remove KCl and excess ligand. All solvent was again removed; diethyl ether (20 mL) was added, and the solid was triturated ultrasonically. The bright yellow product was washed with petroleum ether (10 mL) and dried under vacuum. Yield: 62 mg (78%). IR (solid state): 1641, 1463, 1436, 1397, 1347, 1278, 1221, 1173, 1119, 1096, 979, 919, 831 cm^{-1} ; ^{31}P NMR (acetone- d_6): δ -11.9 (s, dppa) ppm; ^1H NMR (acetone- d_6): δ 4.54 (d, $J_{\text{HH}} = 5.8$ Hz, 8 H; NCH_2), 5.27 (dd, $J_{\text{HBHC}} = 10.1$ Hz, $J_{\text{HBHA}} = 1.4$ Hz, 4 H; $=\text{CH}^{\text{B}}$), 5.30 (dd, $J_{\text{HAHC}} = 17.1$ Hz, $J_{\text{HAHB}} = 1.4$ Hz, 4 H; $=\text{CH}^{\text{A}}$), 5.99 (m, 4 H; $=\text{CH}^{\text{C}}$), 7.50–7.58 (m, 20 H; PPh_2) ppm; MS (FAB +ve) m/z (%) 1133 (1) [M^+], 960 (100) [$\text{M}^+ - \text{S}_2\text{CN}(\text{CH}_2\text{CH}=\text{CH}_2)_2$]; Anal. Calcd (%) for $\text{C}_{40}\text{H}_{40}\text{Au}_2\text{N}_2\text{P}_2\text{S}_4$ ($M_w = 1132.90$): C 42.4, H 3.6, N 2.5. Found: C 42.6, H 3.4, N 2.4.

$[(\text{dppf})\{\text{AuS}_2\text{CN}(\text{CH}_2\text{CH}=\text{CH}_2)_2\}_2]$ (**7**). A solution of $[(\text{dppf})\{\text{AuCl}\}_2]$ (60 mg, 0.059 mmol) in dichloromethane (10 mL) and methanol (5 mL) was treated with 2.2 equiv of $\text{KS}_2\text{CN}(\text{CH}_2\text{CH}=\text{CH}_2)_2$ in water (0.67 mL), and the reaction was stirred for 1 h. All solvent was removed, and the residue was dissolved in the minimum volume of dichloromethane and filtered through diatomaceous earth (Celite) to remove KCl and excess ligand. All solvent was again removed; diethyl ether (20 mL) was added, and the solid was triturated ultrasonically. The pale yellow product was washed with petroleum ether (10 mL) and dried under vacuum. Yield: 61 mg (80%). IR (solid state): 3067, 2904, 1640, 1454, 1434, 1390, 1333, 1281, 1218, 1173, 1102, 1039, 998, 972, 923, 834 cm^{-1} ; ^{31}P NMR (acetone- d_6): δ 30.1 (s, dppf) ppm; ^1H NMR (acetone- d_6): δ 4.49 (m, 4 H; C_5H_4), 4.57 (d, $J_{\text{HH}} = 5.8$ Hz, 8 H; NCH_2), 4.92 (m, 4 H; C_5H_4), 5.25 (dd, $J_{\text{HBHC}} = 10.3$ Hz, $J_{\text{HBHA}} = 1.4$ Hz, 4 H; $=\text{CH}^{\text{B}}$), 5.28 (dd, 4 H; $=\text{CH}^{\text{A}}$), $J_{\text{HAHC}} = 17.2$ Hz, $J_{\text{HAHB}} = 1.4$ Hz), 5.99 (m, 4 H; $=\text{CH}^{\text{C}}$), 7.52–7.74 (m, 20 H; PPh_2) ppm; MS (FAB +ve) m/z (%) 1120 (38) [$\text{M}^+ - \text{DTC}$]; Anal. Calcd (%) for $\text{C}_{48}\text{H}_{48}\text{Au}_2\text{FeN}_2\text{P}_2\text{S}_4$ ($M_w = 1292.90$): C 44.6, H 3.7, N 2.2. Found: C 44.5, H 3.6, N 2.3.

$[(\text{dppm})\{\text{Au}_2\text{S}_2\text{CN}(\text{CH}_2\text{CH}=\text{CH}_2)_2\}]\text{OTf}$ (**8**). $[(\text{dppm})\{\text{AuCl}\}_2]$ (50 mg, 0.059 mmol) and silver triflate (30.3 mg, 0.118 mmol) were dissolved in tetrahydrofuran (10 mL). The reaction was stirred in the dark for 45 min at 0 $^\circ\text{C}$, and then the solution was filtered into a mixture containing the aqueous solution of the diallyl ligand (0.34 mL, 0.065 mmol) and acetone (10 mL). Stirring was continued for 1 h at 0 $^\circ\text{C}$, and then all solvent was removed. The crude product was dissolved in dichloromethane (30 mL) and filtered through Celite. All solvent was again removed, and the residue was triturated ultrasonically in diethyl ether (10 mL) to give a pale yellow product. Yield: 63 mg (97%). IR (solid state): 1482, 1437, 1409, 1256, 1226, 1156, 1100, 1029, 995, 933, 783 cm^{-1} ; ^{31}P NMR (acetone- d_6): δ 33.9 (s, dppm) ppm; ^1H NMR (acetone- d_6): δ 4.70 (d, $J_{\text{HH}} = 5.7$ Hz, 4 H; NCH_2), 4.74 (m, $J_{\text{HP}} =$ unresolved, 2 H; PCH_2P), 5.38 (d, $J_{\text{HBHC}} = 10.1$ Hz, 2 H; $=\text{CH}^{\text{B}}$), 5.39 (d, 2 H; $=\text{CH}^{\text{A}}$, $J_{\text{HAHC}} = 18.0$ Hz), 6.05 (m, 2 H; $=$

CH^{C}), 7.43–7.56, 7.85–7.87 (m \times 2, 20 H; PPh_2) ppm; MS (FAB +ve) m/z (%) 950 (20) [M^+]; Anal. Calcd (%) for $\text{C}_{33}\text{H}_{32}\text{Au}_2\text{F}_3\text{NO}_3\text{P}_2\text{S}_3$ ($M_w = 1099.69$): C 36.0, H 2.9, N 1.3. Found: C 36.1, H 2.9, N 1.2.

$[\text{Au}_2\{\text{S}_2\text{CN}(\text{CH}_2\text{CH}=\text{CH}_2)_2\}_2]$ (**9**). A solution of $[\text{AuCl}(\text{tht})]$ (100 mg, 0.312 mmol) in dichloromethane (10 mL) and methanol (5 mL) was treated with 1 equiv of $\text{KS}_2\text{CN}(\text{CH}_2\text{CH}=\text{CH}_2)_2$ (0.312 mmol) in water (1.60 mL), and the reaction was stirred for 1 h. All solvent was removed, and the residue was dissolved in the minimum volume of dichloromethane and filtered through diatomaceous earth (Celite) to remove KCl and excess ligand. All solvent was again removed; diethyl ether (30 mL) was added, and the solid was triturated ultrasonically. The yellow product was washed with petroleum ether (10 mL) and dried under vacuum. Yield: 140 mg (61%). IR (solid state): 1640, 1468, 1399, 1346, 1330, 1270, 1222, 1164, 1122, 1068, 972, 934, 908, 856 cm^{-1} ; ^1H NMR (benzene- d_6): δ 4.13 (d, $J_{\text{HH}} = 5.6$ Hz, 8 H; NCH_2), 4.90 (d, 4 H; $=\text{CH}^{\text{A}}$, $J_{\text{HAHC}} = 17.1$ Hz), 4.97 (d, $J_{\text{HBHC}} = 10.2$ Hz, 4 H; $=\text{CH}^{\text{B}}$), 5.53–5.63 (m, 4 H; $=\text{CH}^{\text{C}}$) ppm; MS (ES +ve) m/z (%) 739 (2) [M^+], 541 (99) [$\text{M}^+ - \text{Au}$]; Anal. Calcd (%) for $\text{C}_{14}\text{H}_{20}\text{Au}_2\text{N}_2\text{S}_4$ ($M_w = 738.52$): C 22.8, H 2.7, N 3.8. Found: C 22.9, H 2.6, N 3.6.

$[(\text{Ph}_3\text{P})\text{Au}(\text{S}_2\text{CNC}_4\text{H}_6)]$ (**10**). A solution of $[\text{AuCl}(\text{PPh}_3)]$ (200 mg, 0.404 mmol) in dichloromethane (20 mL) and acetone (20 mL) was treated with 1.5 equiv of $\text{KS}_2\text{CNC}_4\text{H}_6$ [generated from 3-pyrroline (46 μL) and CS_2 (44 μL) in the presence of KOH (37 mg)] in water (4 mL), and the reaction was stirred for 30 min. All solvent was removed, and the residue was dissolved in the minimum volume of dichloromethane and filtered through diatomaceous earth (Celite) to remove KCl and excess ligand. All solvent was again removed; diethyl ether (30 mL) was added, and the solid was triturated ultrasonically. The pale orange product was washed with petroleum ether (10 mL) and dried under vacuum. Yield: 205 mg (84%). IR (solid state): 1482, 1400, 1354, 1194, 998, 936, 877 cm^{-1} ; ^{31}P NMR (acetone- d_6): δ 34.1 (s, PPh_3) ppm; ^1H NMR (acetone- d_6): δ 4.49 (s, 4 H; NCH_2), 5.96 (s, 2 H; $\text{CH}=\text{CH}$), 7.57–7.73 (m, 15 H; C_6H_5) ppm; ^{13}C NMR (CD_2Cl_2 , 400 MHz): δ 203.4 (s, CS_2), 134.5 (d, $J_{\text{CP}} = 14.0$ Hz; $o/m\text{-PC}_6\text{H}_5$), 131.8 (d, $J_{\text{CP}} = 1.7$ Hz; $p\text{-PC}_6\text{H}_5$), 130.5 (d, $J_{\text{CP}} = 56.5$ Hz; $ipso\text{-PC}_6\text{H}_5$), 129.4 (d, $J_{\text{CP}} = 11.3$ Hz; $o/m\text{-PC}_6\text{H}_5$), 126.0 (s, CH_2C), 60.7 (s, NCH_2) ppm; MS (ES +ve) m/z (%) 604 (16) [M^+]; Anal. Calcd (%) for $\text{C}_{23}\text{H}_{21}\text{AuNPS}_2$ ($M_w = 603.49$): C 45.8, H 3.5, N 2.3. Found: C 45.8, H 3.4, N 2.4.

$[\text{Au}_2\{\text{S}_2\text{CNC}_4\text{H}_6\}_2]$ (**11**). (a) A solution of $[\text{AuCl}(\text{tht})]$ (50 mg, 0.156 mmol) in dichloromethane (10 mL) and methanol (10 mL) was treated with 1 equiv of $\text{KS}_2\text{CNC}_4\text{H}_6$ [generated as a stock solution as in the synthesis of **10**] in water (2 mL), and the reaction was stirred for 1 h. All solvent was removed; benzene (100 mL) was added to dissolve the relatively insoluble material, and the solid was triturated ultrasonically. The bright orange solid was filtered, washed with water to remove KCl and excess ligand, and dried under vacuum. Yield: 88 mg (83%). (b) Compound **9** (50 mg, 0.068 mmol) and $[\text{Ru}(\text{CHPh})\text{Cl}_2(\text{SiMes})(\text{PCy}_3)]$ (5.9 mg, 0.007 mmol) were dissolved in dry, degassed dichloromethane (30 mL), and this solution was stirred for 2 h. All solvent was then removed, and the residue was triturated in diethyl ether (10 mL) to yield a bright orange product, which was dried under vacuum. Yield: 33 mg (71%). IR (solid state): 2902, 2848, 1447, 1409, 1351, 1173, 1002, 988, 937, 872, 741 cm^{-1} ; ^1H NMR ($\text{dmsO-}d_6$): δ 4.52 (s, 8 H; NCH_2), 6.00 (s, 4 H; $\text{CH}=\text{CH}$) ppm; MS (ES +ve) m/z (%) 680 (2) [M^+], 485 (100) [$\text{M}^+ - \text{Au}$]; Anal. Calcd (%) for $\text{C}_{10}\text{H}_{12}\text{Au}_2\text{N}_2\text{S}_4$ ($M_w = 682.41$): C 17.6, H 1.8, N 4.1. Found: C 17.7, H 1.7, N 4.0.

$\text{AuS}_2\text{CN}(\text{CH}_2\text{CH}=\text{CH}_2)_2$ (**NP1**). An acetone solution (25 mL) of **9** (60 mg, 0.081 mmol) was treated with an aqueous solution (4 mL) of sodium borohydride (30 mg, 0.793 mmol), causing an instant darkening and precipitation of the product. The product was separated by centrifuging and washed repeatedly with water to give a fine black solid. Yield 11 mg (69%, based on material being 97.7% Au). IR (solid state): 1638, 1454, 1385, 1346, 1330, 1290, 1266, 1213, 1166, 1125, 1068, 971, 923, 908, 873, 697 cm^{-1} ; ^1H NMR (benzene- d_6): δ 4.06 (d, $J_{\text{HH}} = 5.8$ Hz, 4 H; NCH_2), 4.94 (dd, $J_{\text{HAHC}} = 17.1$ Hz, $J_{\text{HAHB}} = 1.3$ Hz, 2 H; $=\text{CH}^{\text{A}}$), 4.99 (dd, $J_{\text{HBHC}} = 10.2$ Hz, $J_{\text{HBHA}} = 1.3$ Hz, 2 H; $=$

CH^B), 5.53 (m, 2 H; =CH^C) ppm. TME: analysis of 100 nanoparticles gave a size of 4.8 ± 0.7 nm.

Au@S₂CNC₄H₆ (NP2). An acetone solution (25 mL) of **11** (50 mg, 0.073 mmol) was warmed gently with a heat gun, causing an instant darkening and precipitation of the product. The product was separated by centrifugation and washed repeatedly with water to give a fine black solid. Yield: 12 mg (83%). IR (solid state): 1420, 1339, 1257, 1129, 1079, 993, 936, 877, 809, 705 cm⁻¹; ¹H NMR (acetone-*d*₆): δ 4.36 (s, 4 H; NCH₂), 6.88 (s, 2 H; CH=CH) ppm. TME: analysis of 100 nanoparticles gave a size of 4.0 ± 0.7 nm.

Au@S₂CN(CH₂CH=CH₂)₂ (NP3). An aqueous solution (280 mL) of HAuCl₄ (100 mg, 0.295 mmol) was heated to reflux, and sodium citrate (346 mg, 1.177 mmol) in water (20 mL) was added, causing a darkening of the color. The reaction was stirred at reflux for 10 min and then for a further 15 min at room temperature. A solution of KS₂CN(CH₂CH=CH₂)₂ (0.883 mmol) in water (10 mL) was added dropwise, and the reaction was stirred for a further 3 h. The resulting suspension was left to stand; the supernatant was decanted, and the solid was washed with water (200 mL) to remove excess sodium citrate and ligand. The black solid was dried under vacuum. Yield: 57 mg (98%). IR (solid state): 1676, 1484, 1417, 1348, 1242, 1144, 1038, 941, 760, 648 cm⁻¹; ¹H NMR (acetone-*d*₆): δ 4.41, 4.67 (m \times 2, 2 \times 2 H; NCH₂), 5.27 (m, 4 H; =CH^A + =CH^B), 5.88 (m, 2 H; =CH^C) ppm. TME: analysis of 100 nanoparticles gave a size of 13.7 ± 3.6 nm.

Au@S₂CNC₄H₆ (NP4). (a) An aqueous solution (250 mL) of HAuCl₄ (100 mg, 0.295 mmol) was heated to reflux, and sodium citrate (346 mg, 1.177 mmol) in water (10 mL) was added, causing a darkening of the color. The reaction was stirred at reflux for 10 min and then for a further 15 min at room temperature. A solution of KS₂CNC₄H₆ (0.833 mmol) in a mixture of water (10 mL) and methanol (10 mL) was added dropwise, and the reaction was stirred for a further 3 h. The resulting suspension was left to stand; the supernatant was decanted, and the solid was washed with water (200 mL) to remove excess sodium citrate and ligand. The black solid was dried under vacuum. Yield: 55 mg (95%). (b) Under a nitrogen atmosphere, a suspension of **NP3** (25 mg) was stirred in degassed dichloromethane (20 mL) with [Ru(=CH(C₆H₄OⁱPr-2)Cl₂(SImes))] (2.5 mg, essentially stoichiometric, based on the estimate of surface units used—see below) for 36 h. All solvent was removed, and the residue was washed with cold dichloromethane (2 \times 3 mL) to remove remaining catalyst followed by water (4 \times 3 mL) and dried under vacuum. Yield: 24 mg (quantitative). IR (solid state): 1420, 1339, 1464, 1374, 1345, 1166, 987, 923, 838, 718, 652 cm⁻¹; ¹H NMR (acetone-*d*₆): δ 4.57, 4.76 (m \times 2, 2 \times 2 H; NCH₂), 6.07 (s, 2 H; CH=CH) ppm. TME: analysis of 100 nanoparticles gave a size of 15.0 ± 1.8 nm.

For a nanoparticle with average radius of 6.85 nm (e.g., **NP3**), the number of gold atoms is approximately 125 000, with around 10 000 atoms at the surface.⁵⁹ If there is a surface unit for every four surface atoms, there are 2500 dithiocarbamate units, contributing around 1.7% of the mass of the nanoparticle. A similar value arises from calculations using the “footprint” (obtained crystallographically) of the surface unit and the (widely used) assumption⁶⁰ that around 70% coverage is achieved. This renders the mass of the nanoparticles essentially the same as that of gold, which is used in the yield calculations above.

CRYSTALLOGRAPHY

Crystals of compounds **1** and **9** were grown by vapor diffusion of diethyl ether onto a dichloromethane solution of the complex in each case. Data were collected using an Oxford Diffraction Xcalibur 3 diffractometer, and the structures were refined based on *F*² using the SHELXTL and SHELX-97 program systems.⁶¹

Crystal data for **1**: C₂₅H₂₅AuNPS₂, *M* = 631.52, monoclinic, *P*₂*1**c* (no. 14), *a* = 12.94805(15), *b* = 12.83389(14), *c* = 14.34358(15) Å, β = 91.0548(10)°, *V* = 2383.12(5) Å³, *Z* = 4, *D*_c = 1.760 g cm⁻³, μ (Mo *K* α) = 6.428 mm⁻¹, *T* = 173 K, pale yellow blocks, Oxford Diffraction Xcalibur PX Ultra diffrac-

tometer; 8080 independent measured reflections (*R*_{int} = 0.0237), *F*² refinement, *R*₁(obs) = 0.0180, *wR*₂(all) = 0.0328, 6131 independent observed absorption-corrected reflections [*F*_o > 4 σ (*F*_o)], 2 θ _{max} = 66°, 272 parameters. CCDC 830717.

Crystal data for **9**: C₁₄H₂₀Au₂N₂S₄, *M* = 738.49, tetragonal, *I*₄*1a* (no. 88), *a* = *b* = 18.4430(2), *c* = 22.9755(3) Å, *V* = 7815.0(2) Å³, *Z* = 16, *D*_c = 2.511 g cm⁻³, μ (Mo *K* α) = 15.425 mm⁻¹, *T* = 173 K, yellow needles, Oxford Diffraction Xcalibur 3 diffractometer; 6882 independent measured reflections (*R*_{int} = 0.0376), *F*² refinement, *R*₁(obs) = 0.0242, *wR*₂(all) = 0.0494, 5670 independent observed absorption-corrected reflections [*F*_o > 4 σ (*F*_o)], 2 θ _{max} = 66°, 209 parameters. CCDC 830718.

COMPUTATIONAL METHODS

DFT calculations were carried out on a high-performance computing (HPC) unit using the ab initio software package *Gaussian09*.⁶² The density functional of choice was Perdew–Burke–Ernzerhof (PBE).⁶³ Gold electrons were modeled with the LANL2DZ⁶⁴ basis set (for the 5s²5p⁶5f¹⁰6s¹ valence electrons) and pseudopotential (for the remaining 60 core electrons). For all other elements, a 6-31G(d,p) basis set was used. Using the standard implementation of *Gaussian09*, all molecules discussed in this Work have been optimized to an energetic minimum, and ordinary frequency calculations were carried out on the optimized structures to confirm this. When adsorption of Me₂NCS₂⁻ and ·SMe₂ was studied on pristine gold nanoclusters, ligand molecules were first allowed to optimize on the frozen nanoclusters; only then were gold atoms unfrozen and optimization continued.

All systems were assumed to be in their lowest spin state, and the stability of their calculated wave function was verified prior to calculation of energetic and electronic properties. Charge distribution was calculated using the electro-static potential (ESP) fitting method by Merz, Kollman, and Singh:^{65,66} because of the absence of a default value for the van der Waals radius of gold in *Gaussian09*, the value of 1.66 Å calculated by Bondi was used.^{14b} Default *Gaussian09* values were used for van der Waals radii of the remaining atoms.

ASSOCIATED CONTENT

Supporting Information

This consists of crystallographic data and anisotropic displacement ellipsoid plots for the structures of **1** and **9**. This material is available free of charge via the Internet at <http://pubs.acs.org>.

AUTHOR INFORMATION

Corresponding Author

*E-mail: j.wilton-ely@imperial.ac.uk.

Notes

The authors declare no competing financial interest.

ACKNOWLEDGMENTS

We are grateful to Johnson Matthey Ltd. for a generous loan of gold and ruthenium salts. We would also like to acknowledge the Imperial College High Performance Computing service for providing and hosting the necessary resources for the computational part of this work. We thank Dr. F. Bresme and Dr. M. Bearpark for useful discussions. We gratefully acknowledge the support of the Leverhulme Trust (Grant RPG-2012-634) for a studentship (A.T.).

DEDICATION

Dedicated to the memory of Dr. Joachim Steinke.

REFERENCES

- (1) Samojłowicz, C.; Bieniek, M.; Grell, K. *Chem. Rev.* **2009**, *109*, 3708–3742.
- (2) Nicolaou, K. C.; Bulger, P. G.; Sarlah, D. *Angew. Chem., Int. Ed.* **2005**, *44*, 4490–4527.
- (3) (a) Connon, S. J.; Rivard, M.; Zaja, M.; Blechert, S. *Adv. Synth. Catal.* **2003**, *345*, 572–575. (b) Yang, Q.; Xiao, W.-J.; Yu, Z. *Org. Lett.* **2005**, *7*, 871–874. (c) Binder, J. B.; Blank, J. J.; Raines, R. T. *Org. Lett.* **2007**, *9*, 4885–4888.
- (4) Delépine, M. *Compt. Rend.* **1907**, *144*, 1125–1127.
- (5) (a) Coucouvanis, D. *Prog. Inorg. Chem.* **1970**, *11*, 233–371. (b) Coucouvanis, D. *Prog. Inorg. Chem.* **1979**, *26*, 301–469. (c) Burns, R. P.; McCullough, F. P.; McAuliffe, C. A. *Adv. Inorg. Chem. Radiochem.* **1980**, *23*, 211–280. (d) Hogarth, G. *Prog. Inorg. Chem.* **2005**, *53*, 71–561. (e) Cookson, J.; Beer, P. D. *Dalton Trans.* **2007**, 1459–1472.
- (6) Bond, A. M.; Martin, R. L. *Coord. Chem. Rev.* **1984**, *54*, 23–98.
- (7) (a) Wilton-Ely, J. D. E. T.; Solanki, D.; Hogarth, G. *Eur. J. Inorg. Chem.* **2005**, 4027–4030. (b) Knight, E. R.; Solanki, D.; Hogarth, G.; Holt, K. B.; Thompson, A. L.; Wilton-Ely, J. D. E. T. *Inorg. Chem.* **2008**, *47*, 9642–9653. (c) Macgregor, M. J.; Hogarth, G.; Thompson, A. L.; Wilton-Ely, J. D. E. T. *Organometallics* **2009**, *28*, 197–208.
- (8) (a) Knight, E. R.; Cowley, A. R.; Hogarth, G.; Wilton-Ely, J. D. E. T. *Dalton Trans.* **2009**, 607–609. (b) Knight, E. R.; Leung, N. H.; Lin, Y. H.; Cowley, A. R.; Watkin, D. J.; Thompson, A. L.; Hogarth, G.; Wilton-Ely, J. D. E. T. *Dalton Trans.* **2009**, 3688–3697. (c) Knight, E. R.; Leung, N. H.; Thompson, A. L.; Hogarth, G.; Wilton-Ely, J. D. E. T. *Inorg. Chem.* **2009**, *48*, 3866–3874. (d) Hogarth, G.; Rainford-Brent, E.-J. C.-R. C. R.; Kabir, S. E.; Richards, I.; Wilton-Ely, J. D. E. T.; Zhang, Q. *Inorg. Chim. Acta* **2009**, *362*, 2020–2026. (e) Naeem, S.; Ogilvie, E.; White, A. J. P.; Hogarth, G.; Wilton-Ely, J. D. E. T. *Dalton Trans.* **2010**, *39*, 4080–4089. (f) Lin, Y. H.; Leung, N. H.; Holt, K. B.; Thompson, A. L.; Wilton-Ely, J. D. E. T. *Dalton Trans.* **2009**, 7891–7901. (g) Oliver, K.; White, A. J. P.; Hogarth, G.; Wilton-Ely, J. D. E. T. *Dalton Trans.* **2011**, *40*, 5852–5864. (h) Naeem, S.; Delaude, L.; White, A. J. P.; Wilton-Ely, J. D. E. T. *Inorg. Chem.* **2010**, *49*, 1784–1793.
- (9) (a) Naeem, S.; White, A. J. P.; Hogarth, G.; Wilton-Ely, J. D. E. T. *Organometallics* **2010**, *29*, 2547–2556. (b) Naeem, S.; White, A. J. P.; Hogarth, G.; Wilton-Ely, J. D. E. T. *Organometallics* **2011**, *30*, 2068–2069.
- (10) (a) Kello, E.; Lokaj, J.; Vrabel, V. *Collect. Czech. Chem. Commun.* **1992**, *57*, 332–338. (b) Lokaj, J.; Kettmann, V.; Pavelcik, F.; Vrabel, V.; Garaj, J. *Collect. Czech. Chem. Commun.* **1982**, *47*, 2633–2638. (c) Lokaj, J.; Pavelcik, F.; Kettmann, V.; Masaryk, J.; Vrabel, V.; Garaj, J. *Acta Crystallogr., Sect. B: Struct. Sci.* **1981**, *37*, 926–928. (d) Kello, E.; Kettmann, V.; Garaj, J. *Collect. Czech. Chem. Commun.* **1984**, *49*, 2210–2221. (e) Okumura, K.; Kouyama, S. J. *Photopolym. Sci. Technol.* **1995**, *8*, 365–368.
- (11) (a) Miller, J. B.; Burmeister, J. L. *Synth. React. Inorg. Met.-Org. Chem.* **1985**, *15*, 223–233. (b) *Gold—Progress in Chemistry, Biochemistry, and Technology*; Schmidbaur, H., Ed.; John Wiley & Sons: New York, 1999.
- (12) (a) Wessels, J. M.; Nothofer, H.-G.; Ford, W. E.; von Wrochem, F.; Scholz, F.; Vossmeier, T.; Schroedter, A.; Weller, H.; Yasuda, A. J. *Am. Chem. Soc.* **2004**, *126*, 3349–3356. (b) Zhao, Y.; Pérez-Segarra, W.; Shi, Q.; Wei, A. J. *Am. Chem. Soc.* **2005**, *127*, 7328–7329. (c) Vickers, M. S.; Cookson, J.; Beer, P. D.; Bishop, P. T.; Thiebaut, B. J. *Mater. Chem.* **2006**, *16*, 209–215. (d) Huff, T. B.; Hansen, M. N.; Zhao, Y.; Cheng, J.-X.; Wei, A. *Langmuir* **2007**, *23*, 1596–1599. (e) Park, M.-H.; Ofir, Y.; Samanta, B.; Arumugam, P.; Miranda, O. R.; Rotello, V. M. *Adv. Mater.* **2008**, *20*, 4185–4188. (f) Hansen, M. N.; Chang, L.-S.; Wei, A. *Supramol. Chem.* **2008**, *20*, 35–40. (g) Cormode, D. P.; Davis, J. J.; Beer, P. D. *J. Inorg. Organomet. Polym.* **2008**, *18*, 32–40. (h) Sharma, J.; Chhabra, R.; Yan, H.; Liu, Y. *Chem. Commun.* **2008**, 2140–2142. (i) Zhu, H.; Coleman, D. M.; Dehen, C. J.; Geisler, I. M.; Zemlyanov, D.; Chmielewski, J.; Simpson, G. J.; Wei, A. *Langmuir* **2008**, *24*, 8660–8666. (j) Subramani, C.; Ofir, Y.; Patra, D.; Jordan, B. J.; Moran, I. W.; Park, M.-H.; Carter, K. R.; Rotello, V. M. *Adv. Funct. Mater.* **2009**, *19*, 2937–2942. (k) Park, M.-H.; Ofir, Y.; Samanta, B.; Rotello, V. M. *Adv. Mater.* **2009**, *21*, 2323–2327. (l) Ichikawa, H.; Yasui, K.; Ozawa, M.; Fujita, K. *Synth. Met.* **2009**, *159*, 973–976. (m) Patel, G.; Kumar, A.; Pal, U.; Menou, S. *Chem. Commun.* **2009**, 1849–1851. (n) Wan, H.; Chen, L.; Chen, J.; Zhou, H.; Liu, L. J. *Dispersion Sci. Technol.* **2009**, *30*, 194–197. (o) Zhao, Y.; Newton, J. N.; Liu, J.; Wei, A. *Langmuir* **2009**, *25*, 13833–13839. (p) Subramani, C.; Bajaj, A.; Miranda, O. R.; Rotello, V. M. *Adv. Mater.* **2010**, *22*, 5420–5423. (q) Duan, X.; Park, M.-H.; Zhao, Y.; Berenschot, E.; Wang, Z.; Reinhoudt, D. N.; Rotello, V. M.; Huskens, J. *ACS Nano* **2010**, *4*, 7660–7666. (r) Park, M. H.; Duan, X. X.; Ofir, Y.; Creran, B.; Patra, D.; Ling, X. Y.; Huskens, J.; Rotello, V. M. *ACS Appl. Mater. Interfaces* **2010**, *2*, 795–799. (s) Park, M.-H.; Agasti, S. S.; Creran, B.; Kim, C.; Rotello, V. M. *Adv. Mater.* **2011**, *23*, 2839–2842. (t) Chen, K.; Robinson, H. D. *J. Nanopart. Res.* **2011**, *13*, 751–761. (u) Wrochem, F.; Gao, D.; Scholz, F.; Nothofer, H.; Nelles, G.; Wessels, J. *Nat. Nanotechnol.* **2010**, *119*, 1–7.
- (13) (a) Wilton-Ely, J. D. E. T.; Schier, A.; Schmidbaur, H. *Organometallics* **2001**, *20*, 1895–1897. (b) Wilton-Ely, J. D. E. T.; Ehlich, H.; Schier, A.; Schmidbaur, H. *Helv. Chim. Acta* **2001**, *84*, 3216–3232. (c) Wilton-Ely, J. D. E. T.; Schier, A.; Mitzel, N. W.; Schmidbaur, H. *Inorg. Chem.* **2001**, *40*, 6266–6271. (d) Wilton-Ely, J. D. E. T.; Schier, A.; Mitzel, N. W.; Nogai, S.; Schmidbaur, H. *J. Organomet. Chem.* **2002**, *643*, 313–323.
- (14) (a) Allen, F. H.; Kennard, O.; Watson, D. G.; Brammer, L.; Orpen, A. G.; Taylor, R. J. *Chem. Soc., Perkin Trans.* **1987**, S1–S19. (b) Bondi, A. J. *Phys. Chem.* **1964**, *68*, 441–451.
- (15) Schmidbaur, H.; Schier, A. *Chem. Soc. Rev.* **2008**, *37*, 1931–1951.
- (16) Mansour, M. A.; Connick, W. B.; Lachicotte, R. J.; Gysling, H. J.; Eisenberg, R. *J. Am. Chem. Soc.* **1998**, *120*, 1329–1330.
- (17) On the basis of a search of the Cambridge Structural Database, version 5.34 (Nov 2012 update).
- (18) Lu, X. M.; Yavuz, M. S.; Tuan, H. Y.; Korgel, B. A.; Xia, Y. N. *J. Am. Chem. Soc.* **2008**, *130*, 8900–8901.
- (19) (a) Martín-Alvarez, J. M.; Hampel, F.; Arif, A. M.; Gladysz, J. A. *Organometallics* **1999**, *18*, 955–957. (b) Bauer, E. B.; Ruwwe, J.; Martín-Alvarez, J. M.; Peters, T. B.; Bohling, J. C.; Hampel, F.; Szafert, S.; Lis, T.; Gladysz, J. A. *Chem. Commun.* **2000**, 2261–2262. (c) Ruwwe, J.; Martín-Alvarez, J. M.; Horn, C. R.; Bauer, E. B.; Szafert, S.; Lis, T.; Hampel, F.; Cagle, P. C.; Gladysz, J. A. *Chem.—Eur. J.* **2001**, *7*, 3931–3950. (d) Horn, C. R.; Martín-Alvarez, J. M.; Gladysz, J. A. *Organometallics* **2002**, *21*, 5386–5393. (e) Bauer, E. B.; Hampel, F.; Gladysz, J. A. *Organometallics* **2003**, *22*, 5567–5580. (f) Shima, T.; Hampel, F.; Gladysz, J. A. *Angew. Chem., Int. Ed.* **2004**, *43*, 5537–5540. (g) Shima, T.; Bauer, E. B.; Hampel, F.; Gladysz, J. A. *Dalton Trans.* **2004**, 1012–1028. (h) Wang, L.; Hampel, F.; Gladysz, J. A. *Angew. Chem., Int. Ed.* **2006**, *45*, 4372–4375. (i) Wang, L.; Shima, T.; Hampel, F.; Gladysz, J. A. *Chem. Commun.* **2006**, 4075–4077. (j) Nawara, A. J.; Shima, T.; Hampel, F.; Gladysz, J. A. *J. Am. Chem. Soc.* **2006**, *128*, 4962–4963. (k) Hess, G. D.; Hampel, F.; Gladysz, J. A. *Organometallics* **2007**, *26*, 5129–5131. (l) Skopek, K.; Gladysz, J. A. *J. Organomet. Chem.* **2008**, *693*, 857–866. (m) Skopek, K.; Barbasiewicz, M.; Hampel, F.; Gladysz, J. A. *Inorg. Chem.* **2008**, *47*, 3474–3476. (n) de Quadras, L.; Bauer, E. B.; Stahl, J.; Zhuravlev, F.; Hampel, F.; Gladysz, J. A. *New J. Chem.* **2007**, *31*, 1594–1604.
- (20) (a) Schmid, G.; Pfeil, R.; Boese, R.; Bandermann, F.; Meyer, S.; Calis, G. H. M.; Van der Velden, J. W. A. *Ber. Bunsen-Ges.* **1981**, *114*, 3634–3642. (b) Schmid, G. *Chem. Rev.* **1992**, *92*, 1709–1727. (c) Weare, W. W.; Reed, S. M.; Warner, M. G.; Hutchison, J. E. *J. Am. Chem. Soc.* **2000**, *122*, 12890–12891.
- (21) (a) Ma, Y.; Zeng, J.; Li, W.; McKiernan, M.; Xie, Z.; Xia, Y. *Adv. Mater.* **2010**, *22*, 1930–1934. (b) Gomez, S.; Philippot, K.; Colliere, V.; Chaudret, B.; Senocq, F.; Lecante, P. *Chem. Commun.* **2000**, 1945–1946. (c) Leff, D. V.; Brandt, L.; Heath, J. R. *Langmuir* **1996**, *12*, 4723–4730.
- (22) (a) Selvam, T.; Chi, K.-M. *J. Nanopart. Res.* **2011**, *13*, 1769–1780. (b) Selvam, T.; Chi, K.-M.; Chiang, C.-M. *J. Nanopart. Res.* **2011**, *13*, 3275–3286.

- (23) Tuchscherer, A.; Schaarschmidt, D.; Schulze, S.; Hietschold, M.; Lang, H. *Inorg. Chem. Commun.* **2011**, *14*, 676–678.
- (24) Vignolle, J.; Tilley, T. D. *Chem. Commun.* **2009**, 7230–7232.
- (25) (a) Corbierre, M. K.; Lennox, R. B. *Chem. Mater.* **2005**, *17*, 5691–5696. (b) Goulet, P. J. G.; Lennox, R. B. *J. Am. Chem. Soc.* **2010**, *132*, 9582–9584. (c) Simpson, C. A.; Farrow, C. L.; Tian, P.; Billinge, S. J. L.; Huffman, B. J.; Harkness, K. M.; Cliffler, D. E. *Inorg. Chem.* **2010**, *49*, 10858–10866. (d) Corbierre, M. K.; Beerens, J.; Lennox, R. B. *Chem. Mater.* **2005**, *17*, 5774–5779. (e) Corbierre, M. K.; Beerens, J.; Beauvais, J.; Lennox, R. B. *Chem. Mater.* **2006**, *18*, 2628–2631.
- (26) (a) Nakamoto, M.; Yamamoto, M.; Fukusumi, M. *Chem. Commun.* **2002**, 1622–1623. (b) Nakamoto, M.; Kashiwagi, Y.; Yamamoto, M. *Inorg. Chim. Acta* **2005**, *358*, 4229–4236.
- (27) (a) Beloglazkina, E. K.; Majouga, A. G.; Romashkina, R. B.; Zyk, N. V.; Zefirov, N. S. *Russ. Chem. Rev.* **2012**, *81*, 65–90. (b) Roy, S.; Pericás, M. A. *Org. Biomol. Chem.* **2009**, *7*, 2669–2677. (c) Wilton-Ely, J. D. E. *T. Dalton Trans.* **2008**, 25–29.
- (28) (a) Turkevich, J.; Stevenson, P. C.; Hillier, J. *Discuss. Faraday Soc.* **1951**, *11*, 55–75. (b) Grabar, K. C.; Freeman, R. G.; Hommer, M. B.; Natan, M. J. *Anal. Chem.* **1995**, *67*, 735–743. (c) Kimling, J.; Mier, M.; Okenve, B.; Kotaidis, V.; Ballot, H.; Plech, A. *J. Phys. Chem.* **2006**, *110*, 15700–15707.
- (29) (a) Vericat, C.; Vela, M. E.; Benitez, G.; Carro, P.; Salvarezza, R. C. *Chem. Soc. Rev.* **2010**, *39*, 1805–1834. (b) Tang, Z.; Xu, B.; Wu, B.; Germann, M. W.; Wang, G. *J. Am. Chem. Soc.* **2010**, *132*, 3367–3374.
- (30) Scholl, M.; Ding, S.; Lee, C. W.; Grubbs, R. H. *Org. Lett.* **1999**, *1*, 953–956.
- (31) (a) Kingsbury, J. S.; Harrity, J. P. A.; Bonitatebus, P. J.; H. Hoveyda, A. J. *Am. Chem. Soc.* **1999**, *121*, 791–799. (b) Garber, S. B.; Kingsbury, J. S.; Gray, B. L.; Hoveyda, A. H. *J. Am. Chem. Soc.* **2000**, *122*, 8168–8179. (c) Gessler, S.; Randl, S.; Blechert, S. *Tetrahedron Lett.* **2000**, *41*, 9973–9976.
- (32) Vougioukalakis, G. C.; Grubbs, R. H. *Chem. Rev.* **2010**, *110*, 1746–1787.
- (33) Jin, R. *Nanoscale* **2010**, *2*, 343–362.
- (34) Walter, M.; Akola, J.; Lopez-Acevedo, O.; Jadzinsky, P. D.; Calero, G.; Ackerson, C. J.; Whetten, R. L.; Grönbeck, H.; Häkkinen, H. *Proc. Natl. Acad. Sci. U.S.A.* **2008**, *105*, 9157–9162.
- (35) Kankate, L.; Turchanin, A.; Golzhauser, A. *Langmuir* **2009**, *25*, 10435–10438.
- (36) Hasan, M.; Bethell, D.; Brust, M. *J. Am. Chem. Soc.* **2002**, *124*, 1132–1133.
- (37) Nadler, R.; Sánchez-de-Armas, R.; Sanz, J. F. *Comput. Theor. Chem.* **2011**, *975*, 116–121.
- (38) Tielens, F.; Santos, E. *J. Phys. Chem. C* **2010**, *114*, 9444–9452.
- (39) Heaven, M. W.; Dass, A.; White, P. S.; Holt, K. M.; Murray, R. W. *J. Am. Chem. Soc.* **2008**, *130*, 3754–3755.
- (40) Akola, J.; Walter, M.; Whetten, R. L.; Häkkinen, H.; Grönbeck, H. *J. Am. Chem. Soc.* **2008**, *130*, 3756–3757.
- (41) Qian, H. F.; Eckenhoff, W. T.; Zhu, Y.; Pintauer, T.; Jin, R. C. *J. Am. Chem. Soc.* **2010**, *132*, 8280–8281.
- (42) Jadzinsky, P. D.; Calero, G.; Ackerson, C. J.; Bushnell, D. A.; Kornberg, R. D. *Science* **2007**, *318*, 430–433.
- (43) Jiang, D.-E.; Tiago, M. L.; Luo, W.; Dai, S. *J. Am. Chem. Soc.* **2008**, *130*, 2777–2779.
- (44) (a) Mariscal, M. M.; Olmos-Asar, J. A.; Gutierrez-Wing, C.; Mayoral, A.; Yacaman, M. J. *Phys. Chem. Chem. Phys.* **2010**, *12*, 11785–11790. (b) Askerka, M.; Pichugina, D.; Kuz'menko, N.; Shestakov, A. *J. Phys. Chem. A* **2012**, *116*, 7686–7693.
- (45) Gruene, P.; Rayner, D.; M. Redlich, B.; van der Meer, A. F. G.; Lyon, J. T.; Meijer, G.; Fielicke, A. *Science* **2008**, *321*, 674–676.
- (46) Li, J.; Li, X.; Zhai, H. J.; Wang, L. S. *Science* **2003**, *299*, 864–867.
- (47) Soulé de Bas, B.; Ford, M. J.; Cortie, M. B. *J. Phys.: Condens. Matter* **2006**, *18*, 55–74.
- (48) Krishnamurthy, S.; Shafai, G. S.; Kanhere, D. G.; Soulé de Bas, B.; Ford, M. J. *J. Phys. Chem. A* **2007**, *111*, 10769–10775.
- (49) Kryachko, E. S.; Remacle, F. *Int. J. Quantum Chem.* **2007**, *107*, 2922–2934.
- (50) Schaaff, T. G.; Shafigullin, M. N.; Khoury, J. T.; Vezmar, I.; Whetten, R. L.; Cullen, W. G.; First, P. N.; Gutierrez Wing, C.; Ascensio, J.; Yacaman, M. J. *J. Phys. Chem. B* **1997**, *101*, 7885–7891.
- (51) Bruce, M. I.; Horn, E.; Matison, J. G.; Snow, M. R. *Aust. J. Chem.* **1984**, *37*, 1163–1170.
- (52) Bailey, J. J. *Inorg. Nucl. Chem.* **1973**, *35*, 1921–1924.
- (53) Schmidbaur, H.; Wohlleben, A.; Wagner, F.; Orama, O.; Huttner, G. *Ber. Bunsen-Ges.* **1977**, *110*, 1748–1754.
- (54) Hill, D. T.; Girard, G. R.; McCabe, F. L.; Johnson, R. K.; Stupik, P. D.; Zhang, J.; Reiff, W. M.; Eggleston, D. S. *Inorg. Chem.* **1989**, *28*, 3529–3533.
- (55) (a) Berners-Price, S. J.; Sadler, P. J. *Inorg. Chem.* **1986**, *25*, 3822–3827. (b) Brandys, M.-C.; Jennings, M. C.; Puddephatt, R. J. *J. Chem. Soc., Dalton Trans.* **2000**, 4601–4606.
- (56) Uson, R.; Laguna, A.; Vicente, J. J. *Organomet. Chem.* **1977**, *131*, 471–475.
- (57) Eggleston, D. S.; Chodos, D. F.; Webb, R. L.; Davis, L. L. *Acta Crystallogr., Sect. C* **1986**, *42*, 36–38.
- (58) de Frémont, P.; Scott, N. M.; Stevens, E. D.; Nolan, S. P. *Organometallics* **2005**, *24*, 2411–2418.
- (59) Following method used by Lewis, D. J.; Day, T. M.; MacPherson, J. V.; Pikramenou, Z. *Chem. Commun.* **2006**, 1433–1435.
- (60) Daniel, M.-C.; Astruc, D. *Chem. Rev.* **2004**, *104*, 293–346.
- (61) *SHELXTL PC version 5.1*; Bruker AXS: Madison, WI, 1997. *SHELX-97*; Sheldrick, G., Ed.; Institut Anorg. Chemie: Göttingen, Germany, 1998.
- (62) Frisch, M. J.; Trucks, G. W.; Schlegel, H. B.; Scuseria, G. E.; Robb, M. A.; Cheeseman, J. R.; Scalmani, G.; Barone, V.; Mennucci, B.; Petersson, G. A.; Nakatsuji, H.; Caricato, M.; Li, X.; Hratchian, H. P.; Izmaylov, A. F.; Bloino, J.; Zheng, G.; Sonnenberg, J. L.; Hada, M.; Ehara, M.; Toyota, K.; Fukuda, R.; Hasegawa, J.; Ishida, M.; Nakajima, T.; Honda, Y.; Kitao, O.; Nakai, H.; Vreven, T.; Montgomery Jr., J. A.; Peralta, J. E.; Ogliaro, F.; Bearpark, M.; Heyd, J. J.; Brothers, E.; Kudin, K. N.; Staroverov, V. N.; Kobayashi, R.; Normand, J.; Raghavachari, K.; Rendell, A.; Burant, J. C.; Iyengar, S. S.; Tomasi, J.; Cossi, M.; Rega, N.; Millam, J. M.; Klene, M.; Knox, J. E.; Cross, J. B.; Bakken, V.; Adamo, C.; Jaramillo, J.; Gomperts, R.; Stratmann, R. E.; Yazyev, O.; Austin, A. J.; Cammi, R.; Pomelli, C.; Ochterski, J. W.; Martin, R. L.; Morokuma, K.; Zakrzewski, V. G.; Voth, G. A.; Salvador, P.; Dannenberg, J. J.; Dapprich, S.; Daniels, A. D.; Farkas, Ö.; Foresman, J. B.; Ortiz, J. V.; Cioslowski, J.; Fox, D. J. *Gaussian09, Revision A.2*; Gaussian, Inc.: Wallingford, CT, 2009.
- (63) Perdew, J. P.; Burke, K.; Ernzerhof, M. *Phys. Rev. Lett.* **1996**, *77*, 3865–3868.
- (64) Hay, P. J.; Wadt, W. R. *J. Chem. Phys.* **1985**, *82*, 299–310.
- (65) Singh, U. C.; Kollman, P. A. *J. Comput. Chem.* **1984**, *5*, 129–145.
- (66) Besler, B. H.; Merz, K. M.; Kollman, P. A. *J. Comput. Chem.* **1990**, *11*, 431–439.